Magnet replacement will require the following work at the magnet interconnects:

- backfill the beam and insulating vacuum sectors with dry nitrogen and cut off beam pipes of the replaced magnet
- open the connection space
- remove super-insulation
- cut all the cryo-pipes and transmission lines of a the magnet to replace
- remove replaced magnet moving it horizontally out of the magnet string
- install new magnet following the repair scenario of magnet installation
- make interconnections as described above.

A reasonable goal for the magnet replacement procedure is to complete it during one 8-hour shift of multi-crew work. Pump-down and leak checking operations may extend this time. The overall magnet replacement time will be dominated by cryogenic warm-up and cool-down.

5.1.8.8 Arc Magnet Alignment

During installation, the 65 m magnet is bent in the horizontal plane to the radial position predefined by the pre-aligned support stands. The force necessary to establish the 1.6-cm sagitta is less than 10 kg. It is assumed that the support stand rough alignment is done with the help of a semi-automated surveying system using available survey monuments in the tunnel.

Arc magnets are ready for final alignment after correction magnets are installed and vacuum pipe interconnections are made. Each magnet must be installed so that the magnet reference center is within ± 0.25 mm from the nominal orbit position. For each magnet, an acceptable roll angle is less than 1 mrad rms or less per adjuster. Conventional optical techniques (theodolites and laser trackers) for alignment have angular errors in the range of 10 microns per meter, corresponding to ± 300 microns at the magnet ends from a setup at the center of the magnet. This would be marginally adequate to meet the magnet alignment specification of 250 microns rms over the length of the magnet. However this accuracy can be exceeded using the hydrostatic leveling and stretched wire techniques described below.

For each magnet there will be a support every 6 meters with horizontal, vertical and roll adjustment capability. The magnets will be built “laser straight” in the factory. The magnets will be installed in the tunnel with a 15.57-mm sagitta over the 65-meter length. The stiffness of the magnet will allow an independent range of motion of approximately ± 3 mm horizontally or vertically at each adjuster. Motions outside this range will require coordinated movements of nearby adjusters. The magnet position will be roughed in using optical techniques along the beam line relative to the internal tunnel network. At each of the support stands there will be a *hydrostatic leveling pot* for vertical alignment, a *capacitive stretched wire pick up* for horizontal alignment, and an *electronic gravity sensor* for roll. As the adjustment screws are turned there will be real time readout of both systems to allow for the positioning of each segment of the magnet. A ±3 cm range of the adjusting screws will be sufficient to put in the sagitta and to compensate for installation errors in the magnet stands as well as drift and settling of the tunnel (± 1 cm maximum) over a 20-year lifetime.

Vertical alignment can be made using a hydrostatic leveling technique, which makes use of fluid-filled containers with capacitive readouts. This technique allows vertical alignment

within ± 100 μm for each magnet. For larger scale, corrections taking into the account non-uniformity in the Earth's gravitational field must be made. This will require careful study of the Geoid and the change in the density of the earth in the region of the machine. Corrections to the vertical can then be imposed on each magnet.

Magnet roll can be adjusted using a technique similar to the one used during leveling of the magnets. It can help to establish a real time display of the roll of the magnet at each adjustment station. Given a base support of 500 mm and a resolution of 2 microns for the hydrostatic levels a roll angle of ±4 micro-radians is achievable. This exceeds the 1 mrad requirement for acceptable vertical closed-orbit distortion.

Horizontal alignment is done using the stretched wire technique. A small diameter (less than 1 mm) copper beryllium wire mechanically attached to both ends of the magnet forms the reference base. Two wires separated vertically can be used to increase the signal to noise ratio. Using capacitive pickup electrodes at each support stand, it will be possible to adjust horizontal position of each magnet to the desired accuracy. Alignment of the entire 65-meter magnet to within ±100 microns should be possible. To set the sagitta of 15.6 mm for the magnet all the adjustments must be made at the same time. Starting with optical tooling the rough sagitta can be set to an accuracy of ±300 microns. Once this is done the stretched wire system can be installed. Each capacitive pick up will have a different offset from the magnet to account for the sagitta. The final adjustment will involve moving all adjusters at the same time.

A degree of automation is possible. The simplest approach is for the person at the central display of magnet alignment data to give directions to one or more workers with wrenches. A more sophisticated alternative is to manually place motorized wrenches at each of the adjusters, then run automated software procedures to bring the entire magnet into alignment. If these systems were permanently installed and coupled with motorized adjustment stands they could be used as an active alignment that continually aligns the magnets as the machine runs. Beam position monitor information could also be used.

5.1.8.9 Straight Sections and Transfer Line Installation

Special magnets of several types are to be installed in the ten straight sections and two beam injection lines (see Section 5.1.5). Straight section focusing quadrupoles and injection line dipole and Lambertson magnets are conventional magnets. The maximum weight of these magnets does not exceed 5 tons and their length is less than 6 meters, so they are installed on their support stands using conventional techniques.

Separation/recombination dipoles and the abort Lambertson use the transmission line for excitation. To minimize labor related to cryo interconnections, these magnets are assembled in the tunnel by installing steel magnet cores around preinstalled transmission line and vacuum pipes. Individual pieces have lengths up to 6 meters and weigh less than 5 tons. Dipole alignment is non-critical but the Lambertson septa must be accurately aligned.

Pulsed injection and abort kicker magnets and abort sweep-magnets are of dipole type, so installation and alignment procedures for these magnets are straightforward.

Finally there are eight 10-meter, superconducting, high gradient, low-beta IR quadrupoles described in 5.1.4. Each quadrupole will weigh about 25 tons and is rigid enough to be transported to the place of installation using two high load trailers and two transport vehicles of

the type used for the arc magnet transportation. The alignment requirement for these quadrupoles is ±100 μm so two adjustable support stands will be used. The alignment procedures are complicated by the presence of the detectors and could be similar to those used at the LHC.

Because sections that use special magnets are located closer to the Fermilab and Far Side sites than accelerator arcs, installation of these magnet can be done independently of the installation of arc magnets.

5.1.8.10 Installation Schedule

The number and size of working crews needed to install the magnet in a 3-4 year term has been estimated.

At least two access points at the opposite sides of the ring are required. The simplest magnet delivery scenario can be realized when assembly starts from the middle of the half-arcs connecting Fermilab site and Far End site and goes in four directions simultaneously. If magnet replacement is required after the magnet string is installed, a more complicated scheme must be used. In this case magnet traffic will go down the tunnel with already installed magnets, and additional measures must be taken to allow parallel work of an assembly crew. The magnet installation procedure in this case also is more complicated because it requires magnet movement across the tunnel.

Because of a high average magnet transportation distance inside the tunnel (about 30 km), only one magnet per day can be installed by each installation vehicle. Several crews must work simultaneously to make the total installation time acceptable. Connection of the installed magnets in a string can be made simultaneously for several magnets.

5.1.8.11 System Commissioning

The described procedure will ensure interconnections of a high quality; nevertheless, after each 20-km magnet string assembly is completed, a cryo-test must be performed. This cryo-test will involve a pressure test, relief valve setting tests, magnet string cooling down, heat leakage test, and transmission line current test. Cold vacuum leaks could be detected at this point. Cryogenic plant performance and magnet string quench tests will be also conducted.

A temporary installation of the 100-kA holding supply and current leads (Figure 5.42) easily fits in the underground caverns eventually intended for the Stage-2 dump resistors. The 2.5-V holding supply will ramp a 20-km magnet string to 100 kA in 40 minutes. This allows full-current testing of a complete quench protection cell of the accelerator.

The beam pipes are interconnected after the cryogenic test passes and the correction magnet block is installed. Because the system is not baked *in situ*, the static vacuum will improve steadily over time and it is desirable to have most of the system under vacuum for as long as possible before collider ring commissioning.

5.2 Accelerator Systems

The systems distributed around the ring circumference include cryogenics, arc instrumentation, corrector power supplies, and beam vacuum systems. The “once per turn” systems are located primarily in the straight sections on the Fermilab site. These include RF, injection, extraction, and once-per-turn instrumentation.

A completely conventional approach is taken to the standard utilities in the straight sections. Warm iron/copper magnets use LCW cooling and standard power supplies. Electronics and major power supplies are located in underground shielded instrumentation rooms that are accessible with beam on. A larger tunnel, conventional power systems, and generous cable trays provide the infrastructure for RF systems, injection and extraction kickers and Lambertsons, beam crossovers, beam halo scraping, beam current and beam profile monitoring. Concentration of these major subsystems at the Fermilab site makes maintenance and accessibility requirements similar to other Fermilab accelerators. These systems are modeled on existing designs from recent projects for which the specifications and costs are well known.

Four distributed systems contain notable new features which will be described in some detail: the cryogenic system which is smaller and simpler than comparable systems, the beam stop which must deal with the large kinetic energy in the beam, the arc instrumentation which is distributed as electronics modules in “holes in the wall” at each quad location, and the beam damper system which is distributed around the ring circumference.

5.2.1 Cryogenic System

5.2.1.1 Cryogenic System Description

The magnet’s superconducting transmission line is cooled by pressurized supercritical helium at 4.5-6.0 K. The heat load of the magnet system is removed by the sensible heat of the supercritical helium stream. The fluid operates just outside the critical region expanding the helium stream as it passes through the transmission line producing a large effective heat capacity. The tunnel cryogenics are an all-piping system with very simple topology. Figure 5.36 shows the temperature profile in the transmission line.

A rough comparison of the cryogenics of various machines, normalized to beam energy, is given in Table 5.18. For this comparison, the refrigeration for the SSC operating at $L=10^{34}$ was crudely estimated by tripling the dynamic heat load (~2x overall increase). The VLHC-1 cryogenic system is significantly simpler and lower-powered than the LHC or SSC systems.

Table 5.18. Comparison of cryogenics per TeV beam energy for various machines.

		Tevatron	**HERA**	**LHC**	**SSC(10^{33})**	**SSC(10^{34})**	**VLHC-1**
Refrigeration (4.5 K eqv.)/TeV	kW/TeV	27	38	21	10	20	4
Helium Inventory/TeV	tons/TeV	4	21	14	16	16	4
Cold Mass/TeV	tons/TeV	600	5,000	5,143	5,000	5,000	286
Magnetic Stored Energy/TeV	MJ/TeV	400	1,000	1,629	600	600	171

As shown in Figure 5.35, cryogens are fed from six refrigerator plants spaced at 38 km intervals around the ring. For efficiency reasons, refrigeration is provided at two temperature levels. Refrigeration at a higher temperature range (40-70 K) provides cooling for a heat shield that is used to intercept much of the heat that would otherwise be absorbed by the lower temperature superconductor. Each plant provides refrigeration for an upstream and downstream magnet string 19 km long. Each string is sub-divided into two loops, referred to as “near” and “far” loops.

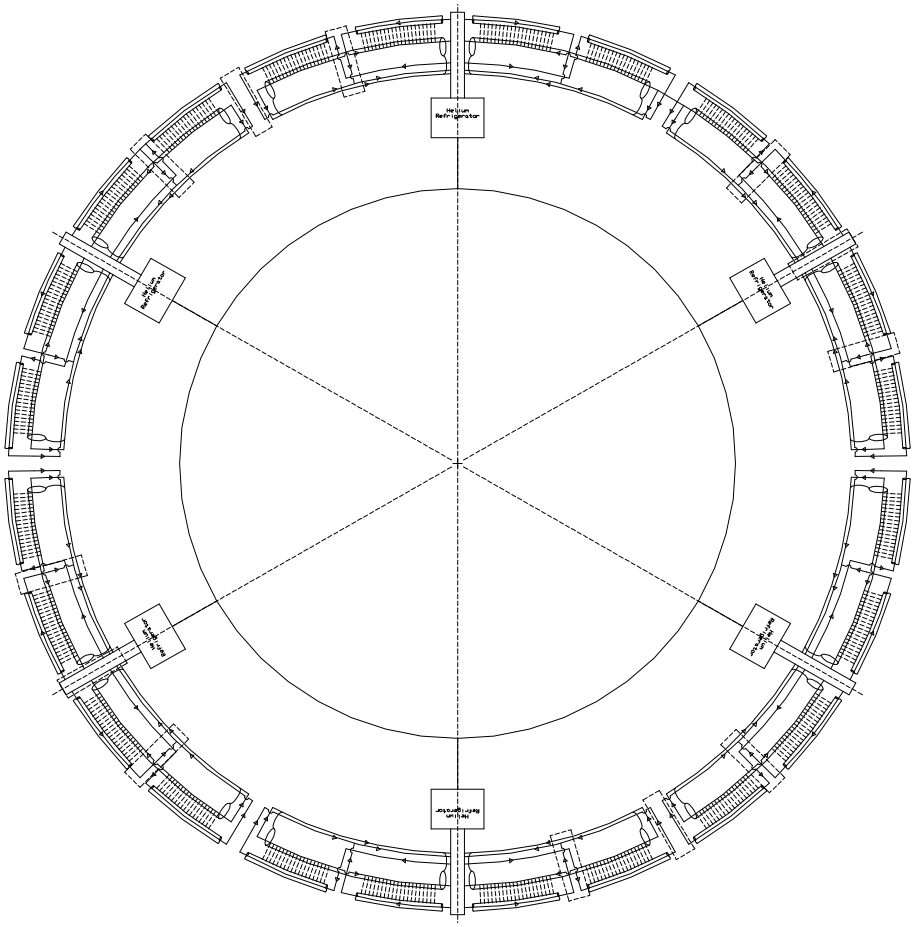

Figure 5.35. Cryogenic layout of the Stage-1 VLHC. Six plants are spaced at 38-km intervals around the ring. Each plant provides refrigeration equivalent to 9.6 kW at 4.5 K. Nominal operating wall power is 2 MW at each plant. One plant is on-site at Fermilab and has additional capacity for detectors, IRs, RF, and superconducting current leads.

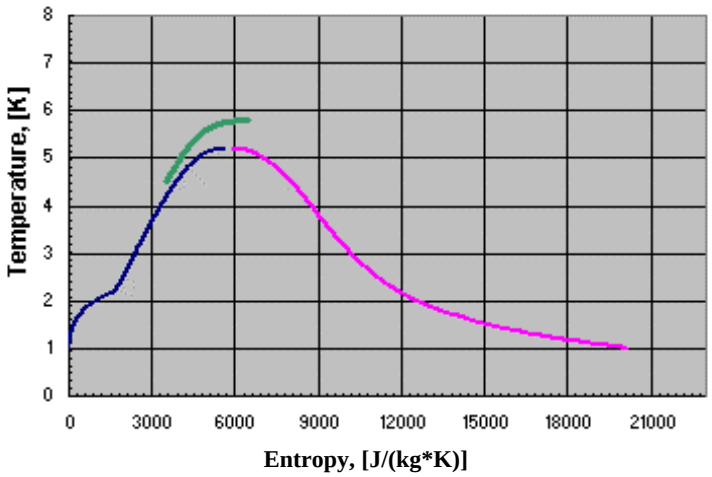

Figure 5.36. Temperature profile of the supercritical flow in the VLHC transmission line.

5.2.1.1.1 Helium Distribution System

The helium distribution system is designed to distribute refrigeration to the magnet system with a minimal temperature variation. The distribution system consists of cryogenic valve boxes, transfer lines, and warm helium header.

Cryogenic Valve Boxes

Cryogenic valve boxes are used to redistribute the helium between the conductor loops for steady-state operation and perform various transient state operations. These boxes are located every 9.5 km and house the control valves and instrumentation required for each circuit. Boxes vary in configuration dependent upon location in the magnet string. These boxes are relatively simple devices mainly providing a transition for flow redistribution.

Transfer Lines

Transfer lines are a part of the magnet assembly. A line contains five circuits: 4.5 K superconductor supply line (near loop only), 6.0 K superconductor return line, 40 K shield supply line, 70 K shield return line, and a vacuum circuit. Each section of transfer line is equal in length to a magnet (67.5 meters) and is attached to the magnet assembly via a structural anchor at the midpoint of the magnet.

- The 70 K return line is a 0.102 m OD stainless steel pipe connected to an extruded aluminum shield that surrounds all the inner lines. The shield is wrapped with double-sided aluminized Mylar (dimpled and perforated). The longitudinal contraction of the line is compensated with guided formed bellows in the interconnects. During this shrinkage, the G-10 support structure is allowed to move within the vacuum space.
- The 40 K shield supply line is a 0.089 m OD stainless steel pipe supported on the G-10 spiders from the aluminum shield. Bellows are used at the end of each 67.5 m module to compensate for thermal contraction and expansion.

- The 4.5 K supply (near loop only) and 6.0 K super conductor return line are Invar tubes that are also anchored at the midpoint of the module. These lines are of concentric design. The 6.0 K helium flows between two concentric Invar tubes
- The 4.5 K supply line is suspended via G-10 spiders from a 6.0 K inner line.

5.2.1.1.2 Helium Pressure Relief and Venting System

Relief valves for each of the five circuits are located every 540 meters, as seen in Figure 5.37. These valves will vent into the warm helium header that is itself protected every 1 km at 3 MPa (30 bar) from over pressurizing. Each relief is conventional in nature and set to the MAWP of its given circuit. The primary need for these reliefs are for trapped volume and loss of insulating vacuum scenarios. The warm header is further protected at the refrigerator (above ground) at a set pressure of 0.2 MPa (2 bar), venting to the atmosphere.

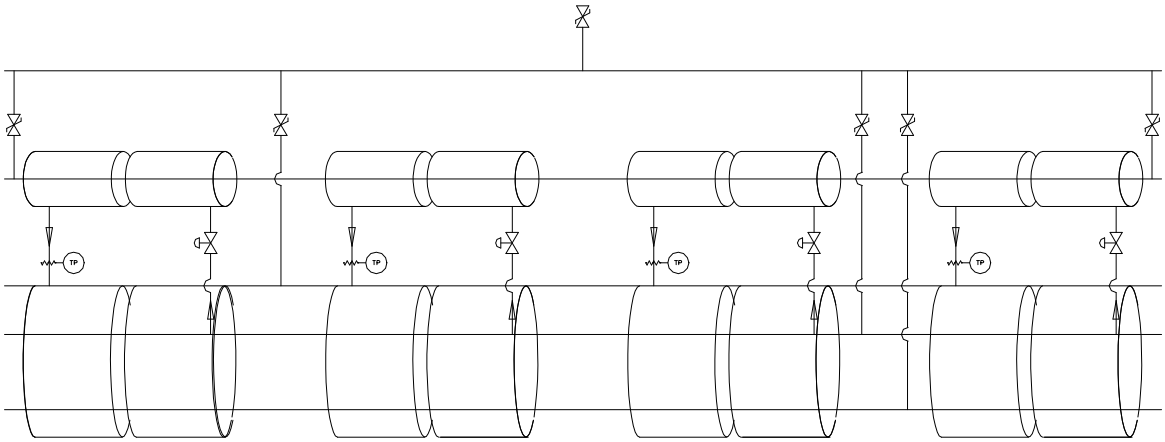

Figure 5.37. Helium shield flow and pressure relief valves.

Quench protection of the transmission line is discussed in Sections 5.1.2.2 and 5.2.2.3. The 100 kA transmission line conductor contains enough copper that it can be safely shut down with a 1 second time constant following a quench. A number of detailed quench simulations have been performed. The peak temperature is ~250 K. The worst-case peak pressure comes from a situation in which a mis-steered beam (kicker misfire) causes the beam to oscillate side-to-side in the beam pipe and scrape heavily in a series of locations separated by a half-betatron wavelength. In this case the peak temperature is unaffected, but a worst-case pressure occurs when the hydrodynamic shock waves from two adjacent quenches collide at the midpoint between quenches. The peak pressure is below the 4 MPa (40 Bar) pressure rating of the transmission line. Thus no helium needs to be vented anywhere, even for a long period following the quench. The pressure burst from the hydrodynamic shock wave, as registered on pressure sensors along the transmission line, should provide a convenient method of identifying where the quench occurred.

5.2.1.1.3 Heat Shield Cooling System

Pressurized 40 K helium is used to intercept the radiation and conduction heat leak to the transmission line. Helium is supplied from the refrigerator at 1.7 MPa (17 bar) and returns at less then 70 K and 1.3 MPa (13 bar). Flow is supplied via a 0.089 m OD tube and distributed via a pair of 6 mm OD lines every 270 meters carrying 2.0 g/sec. This scheme provides shield cooling for every two magnets. Control valves and temperature sensors are included every 270 meters for heat shield flow control based on temperature requirements.

5.2.1.1.4 Transmission Line Heat Load Estimates

Transmission line heat load estimates are divided into two components: the primary heat load on the 4.5 K system and the heat load to the 40 K shield system. The calculated heat loads are presented in Table 5.19.

Table 5.19. VLHC design study calculated transmission line heat loads.

			Primary 4.5K	**Secondary 40K**
STATIC				
	Near Loop			
		Mechanical Supports, [mW/m]	53	670
		Superinsulation, [mW/m]	15	864
	Far Loop			
		Mechanical Supports, [mW/m]	53	670
		Superinsulation, [mW/m]	13	864
DYNAMIC				
		Beam Loss, [mW/m]	2	1
		Superconductor Splice, [mW/m]	7	-

5.2.1.1.5 Cryogenic Loads for On-Site Refrigeration Plant

The extra loads for the on-site refrigeration plant are summarized in Table 5.20. The total refrigeration power (4.5 K equivalent) is comparable to a single additional cryo plant.

Table 5.20. Extra loads for the on-site refrigeration plant.

	4.5 K (static)	**4.5 K (dynamic)**	**40 K (shield)**	**Liquefaction (g/s)**
Current Leads (Sec. 5.2.2.2)	-	-	-	15 g/s
IR Beam Debris (Sec. 5.1.4.2)	-	2.4 kW	0.5 kW	
IR Static Heat Load (rough est.)	0.5 kW	-	10 kW	
RF Cavities (Sec. 5.2.6)	0.48 kW	1.76 kW	-	
On-site Transfer Lines (6 km)	0.2 kW	-	12 kW	
TOTAL	1.2 kW	4.2 kW	25 kW	15 g/s

It is notable that most of the on-site cryogenic loads are dynamic and are not present during the injection cycle when the Tevatron is ramping. It is therefore plausible that most or all of the on-site cryogenic load could be serviced by load shifting from the existing Fermilab Central Helium Liquefier.

5.2.1.1.6 Refrigeration System

The refrigeration system is composed of six 4.5 kW at 4.5 K capacity facilities equally spaced around the ring. Each plant will also provide 100 kW of 40 K refrigeration used in the shielding of the magnet system.

This provides approximately a 50% margin above predicted steady state requirements. This margin is required to ensure continued operation when the heat load increases either due to events such as a magnet quench or vacuum leak, or because refrigeration capacity falls below its intended design value (i.e. decreasing machine efficiency or inefficient heat transfer due to contamination). With this scheme, all six refrigerators must be operational for the accelerator to function. No plant redundancy is built into this design.

Figure 5.38 shows the refrigeration process schematic. The process helium is compressed from suction pressure of 0.101 MPa (1.01 bar) up to an intermediate pressure of 0.4 MPa (4.0 bar) by means of a first stage compressor discharging into a second stage, which compresses the helium to 1.85 MPa (18.5 bar). Turbo machinery is used for the refrigeration plants while positive displacement machines comprise the compressor system. There are two cold boxes: the upper and lower cold boxes. Each cold box contains five plate-and-fin type heat exchangers and three expanders. To avoid return helium gas instabilities due to the elevation change from the tunnel to the surface, the lower cold box will be located at the tunnel level. This requires a dedicated space of 432 m^3 (6 m along the beam by 6 m transverse by 12 m high) located near the accelerator tunnel.

These plants are well within existing commercial vendor capabilities. They are simpler but technologically similar to those of LEP, LHC, SNS, and HERA, and contain no nitrogen pre-cooling. The cold box configuration is a horizontal carbon steel shell enclosure housing all heat exchangers, piping, valves, cold ends of turbo expanders and vessels operating at cryogenic temperatures. The equipment within the cold box and the inner face of the vacuum jacket are covered by multi layer aluminized Mylar. The cold boxes are designed to withstand the outside atmospheric pressure while they are evacuated and are also protected against overpressure by safety valves. All internal valves, filters, turbo expanders, bayonets and major pipe connections are fixed at the top plate and are accessible from a structural steel platform along the length of the cold box.

The turbo expanders are self activated gas bearing type, superior in their performance to oil bearing turbines. Each turbo expander is a small single-stage centrifugal turbine braked by a direct-coupled, single stage centrifugal compressor. The turbine housing is vertically mounted to a plate at the cold box top, projecting into its vacuum space. Within the cold box are brazed aluminum heat exchangers, pressure vessels containing an adsorbent to remove impurities and the cold end of gas-bearing turbo expanders. Part of the outer shell cover is flanged and has an O ring seal, and is removable for complete access to all cold box internal components and piping. Two panels will be mounted on the structural steel platform next to the cold box, one containing all instrument terminations and transmitters, and the other an assembly of purge and

defrost valves. Provisions for purification of the process helium is provided at each plant as well as oil removal systems. A commercial control system package will permit the unattended operation of these plants.

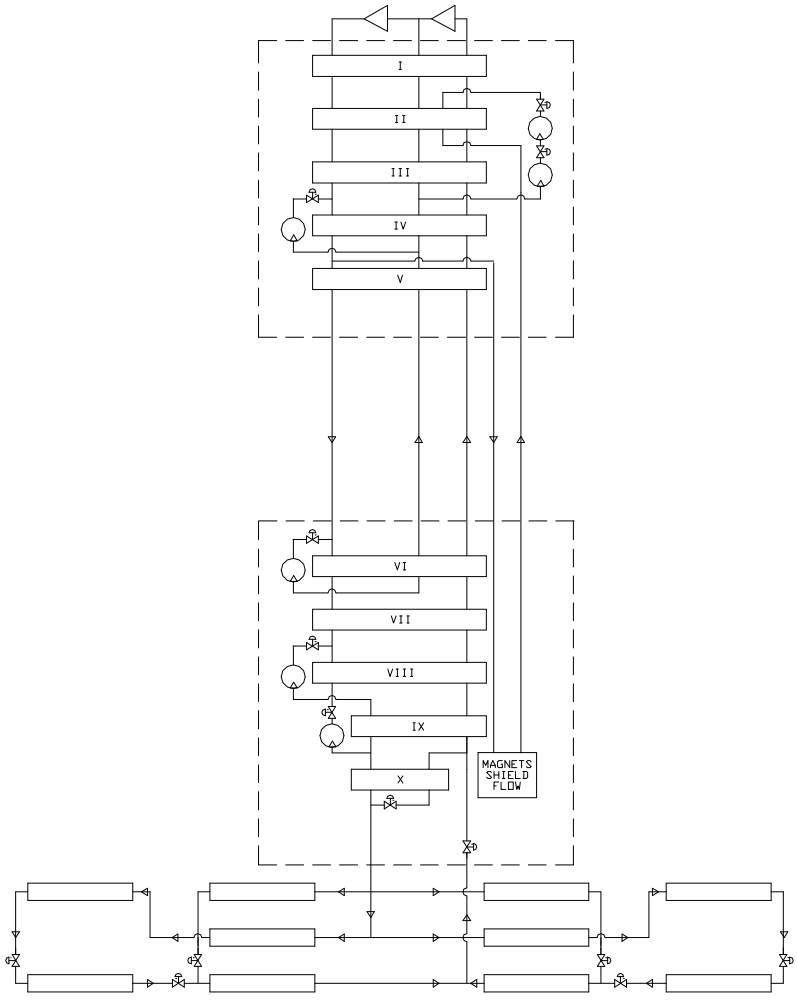

Figure 5.38. Refrigeration process flow and transmission line flow schematic. A split cold box similar to LEP is used to make the process insensitive to altitude changes between the tunnel and surface. The transmission line flows extend ±19 km from the cryo plants. The flow is split into two parallel loops: the "near" loops that extend ±9.5 km from the cryo plant, and the "far" loops that service magnets between 9.5 km and 19 km from the cryo plants.

Table 5.21. Predicted power requirements for ring cryogenics.

		Magnets				Shield
		Transmission Line		Current Return Bus		
		Near Loop	Far Loop	Near Loop	Far Loop	
Temp in	[K]	4.50	4.52	5.44	5.40	37.00
Press in	[bar]	4.00	3.80	2.00	2.50	17.00
Enthalpy in	[J/g]	12.09	12.09	33.92	27.18	207.28
Entropy in	[J/(g*K)]	3.52	3.56	8.19	6.69	14.76
Temp out	[K]	5.57	5.39	5.80	5.54	70.00
Press out	[bar]	2.80	2.50	1.90	2.10	13.00
Enthalpy out	[J/g]	26.40	26.66	37.79	34.24	381.66
Entropy out	[J/(g*K)]	6.44	6.59	8.96	8.18	18.71
Predicted heat load	[W/m]	0.044	0.044	0.024	0.022	1.534
Distance	[m]	19400	19400	19400	19400	38800
Design total heat	[kW]	0.85	0.85	0.47	0.43	60
Mass flow	[g/sec]	60	59	120	60	341
Design ideal power	[kW]	103	107	27	53	345

		Magnets	*Shield*
Predicted heat load	[kW]	2.6	60
Heat uncertainty factor	[-]	1.25	1.25
Design Heat Load	[kW]	3.2	74
Design mass flow	[g/sec]	120	348
Design ideal power	[kW]	291	345
4.5 K equiv design power	[kW]	4.43	5.26
Efficiency (fraction Carnot)	[-]	0.28	0.28
Nominal operating power	[kW]	1039	1233
Overcapacity factor	[-]	1.3	1.3
Installed operating power	(kW)	1351	1603

Operating wall plug power for one sector (MW)	2.0
Installed wall plug power for cryogenics for one sector (MW)	3.0
Operating wall plug power for cryogenics for entire accelerator (MW)	11.8
Installed wall plug power for cryogenics for entire accelerator (MW)	17.7

5.2.1.1.7 Helium Compressor System

The compression package will consist of three oil flooded rotating screw compressors. One compressor will compress from 0.11 MPa (1.1 bar) to 0.4 MPa (4.0 bar), and the two other will compress in parallel from 0.4 MPa (4.0 bar) to 1.85 MPa (18.5 bar). The first stage compressor is smaller than the two second stage machines. Each compressor skid contains the compressor, main drive motor, oil reservoir/separator vessel, and lubrication system mounted on a common rigid skid base. The base plate provided is suitable for installation on a flat pad without grouting. The helium enters the compressor and is compressed through the rotating screw compressor, also flooded with oil. The oil seals the rotor and absorbs some heat of compression. The compressed warm helium passes through a water-cooled heat exchanger and then into a bulk oil separator. The oil is also passed through a separate water-cooled heat exchanger. Each compressor is direct driven by an electric induction electric motor. The compressor assemblies are equipped with automatic inlet and outlet block valves and automatic recycle valves.

The high-pressure helium from the compressors passes through a skid mounted oil removal system. The oil removal system consists of three stages of coalescing filter housings followed by a vessel containing activated carbon. All entrained oil is filtered out of the gas stream by the three stages of filters. The small amount of oil in the vapor phase is removed by the activated carbon. The total amount of oil contained in the helium leaving the oil removal assembly is less than 10 ppb.

5.2.1.1.8 Helium Liquid and Gas Storage and Inventory Management

The inventory for the entire cryogenic system is estimated to be 75 tons of liquid helium, which is twenty times the Tevatron inventory. Each cryogenic plant will have three 37.8 m^3 liquid helium storage dewars, and fifteen gas tanks capacity of 113.6 m^3. This will provide 143 percent of the total helium inventory. The gas storage serves as make-up/kick back during normal operations, and as a buffer/storage during quenches and warm up of a single loop. The liquid storage station will have pumps and heat exchangers necessary to liquefy/warm up cold gas during upset conditions. During the planned warm-up of the entire ring, the inventory will be liquefied into the dewars. In case of a sector warmup, the inventory can be distributed between five sector gas/liquid storage vessels via the cooldown header. The tunnel transfer line and the cooldown header can be used to hold up to 40% of inventory at pressure below the MAWP of any component in the system.

5.2.1.1.9 Cryogenic Control System

A well-proven process control system will be used. The cryogenic system in each sector will be controlled by a commercially available distributed control system (DCS). Commercial program logic controllers will be used for local control of the cryogenic hardware in the event that a high-speed network connection is unavailable. The cryogenic control system will provide full automation of any operation mode, including transient modes. The accelerator high-speed network will be used for communication and data exchange between sectors.

5.2.1.2 Design Operating Conditions

5.2.1.2.1 Steady State

Helium is supplied from a refrigerator at 4.5 K, 0.4 MPa (4 bar) and returned at 5.8 K, 0.19 MPa (1.9 bar). Supercritical supply helium is fed from the helium plant to four parallel loops. Each loop is comprised of 9.5 km of magnet and transmission line. There are cryogenic connecting boxes at the beginning and end of each 9.5 km section. At the exit of the refrigerator the helium process is split into four paths. There are upstream and downstream magnet strings that are mirror images of each other. The typical flow schematic of a magnet string is shown in Figure 5.39.

As helium enters the upstream or downstream magnet strings the flow is split into two parts: half enters the 4.5 K transmission line circuit (for the near loop) and half enters the 4.5 K current return circuit contained in the magnet (for the far loop). There is expected to be an approximately 1 K gradient across each loop. These loop flows are then re-distributed at valve boxes and become the return 6.0 K flow.

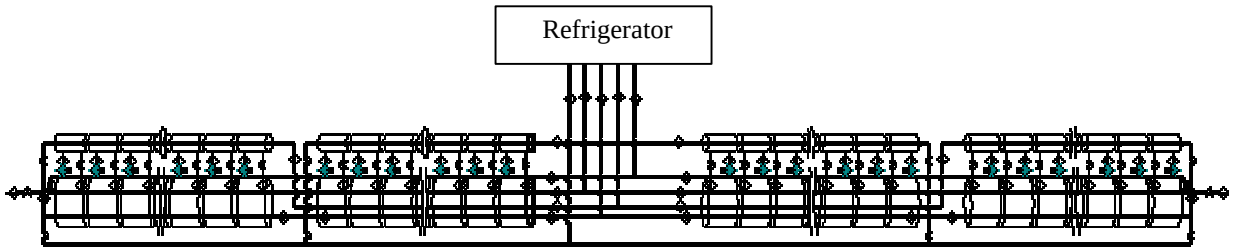

Figure 5.39. Flow schematic of the 38-km sector serviced by one cryogenic plant.

The cooling scheme relies on a balance between heat leak and pressure drop. Any scenario causing an upset in the heat load (i.e. vacuum degradation) can be compensated by increasing the helium flow rate and supply pressure for the proper loop. The refrigerator has been oversized by 50% to compensate for these types of upset conditions.

5.2.1.2.2 System-Wide Purification

Purification of this machine will be done in two steps. First, each sector will be pumped and backfilled five times to 25 inches of mercury via pumpouts on every helium circuit at each valve box located every 10 km. This method has been proven to work in the Tevatron. Levels of contamination less than 100 ppmv are achieved with this first step by using roughing pumps. The second step is dilution purification. A purifier with a nitrogen cooled charcoal bed will be located at each refrigeration plant. The discharge gas of the compressor system will be circulated through this purifier and then will be distributed to the magnet/transmission line system. Contamination instrumentation, such as arc cells used on the Tevatron, will be used to monitor the ppmv levels in each sector. The system will be ready for cool down when contamination levels are < 5 ppm. It is estimated that the purification for a sector in the VLHC will be 72 hours.

5.2.1.2.3 System-Wide Cool down

Cool down of the VLHC will be done in three stages. The first stage involves the cool down of the helium plants. The second stage is the cool down of the transmission line to 40 K. Finally the transmission line will be cooled to operating temperatures.

In the first stage, cooling is provided by turbines and should not take more than 24 hours per plant. In the second stage, the plant is set up in the liquefaction mode and 40 K gas at 0.4 MPa (4 bar) is sent via cool down valves located at each valve box back to the compressor suction warm gas header located in the tunnel. Gas flows out from the refrigerator through the near loop transmission line, the 6.5 K return, the current return bus, and the shield circuits, and then returns via the warm header. When the temperature at the end of the “near” loop (measured at the valve box) is 70 K the flow is then re-directed to the “far” loop and into the return header. As the “far” loop temperature reaches 70 K the second cooldown stage can be started.

During the third cool down stage, the plant is re-tuned for an outlet temperature of 4.5 K. The flow pattern for the second stage is the same as the first stage. As the temperature for each loop is at 7 K the cool down valves can be closed and the flow will be looped back in refrigerator mode. Total cool down time is expected to be on the order of 10 days.

5.2.2 Magnet Power Supplies, Current Leads, and Quench Protection

Stage-1 power supplies are summarized in Table 5.22 below. The major item is the single 100 kA supply for the transmission line magnets. The Interaction Region power supplies, current leads and quench protection are discussed in Section 5.1.4. Total Stage-1 power supply requirements (both ramping and steady state) are about a third of the Fermilab Main Injector.

Table 5.22. Power supply, current leads and quench protection summary for the Stage-1 machine.

	Transmission Line Power Supply	IR Quadrupole Power Supplies (Sec. 5.1.4)	Straight section Warm Magnet Power Supplies	Corrector Magnets (warm copper)
Number	1	2	16 approx.	12,000
Location	FNAL	at Experiments	Straights	Quad locations
Voltage per supply	62	10 V typ.	1000 V typ.	100 Typ
Current per supply	100 kA	25 kA	200 A typ	2 A typ
Ramping MVA (tot)	6.2 MVA	1 MVA	-	-
DC Power (total)	0.4 MW	0.6 MW	7.4 MW	2.1 MW
LCW Consumption	-	-	150 liters/sec	*(air cooled)*
Quench Detection	1 Circuit at PS	2 circuits/quad	-	-
Quench Protection	Dumps @ 20 km	4 heaters/quad	-	-
SC Current leads	100 kA-pair	60 kA-pair	-	-
Peak Ramping Supply Power	**17.7 MW**			
Total Power Supply Power in Collision	**10.5 MW**			

5.2.2.1 Main Transmission Line Power Supply

The low inductance (3 μH/m, 0.6 H ring total) and low stored energy (10 kJ/m, 3 GJ total) of the single-turn transmission line magnet allow the entire ring to be powered from a single supply [50]. See Figure 5.40. A voltage of ±62 V ramps the machine up or down in 1000 seconds. The design current of 100 kA at flattop exceeds the 87.5 kA required for the transmission line magnet to reach its design field. The supply will be located on site at Fermilab in a shielded underground room approximately 25’ x 50 ft in size. The ramping power and footprint of the power supply is comparable to one of the six Main Injector power supply buildings. Superconducting current leads will be located immediately adjacent to the supply to minimize power loss in warm buswork. Superconducting buswork will carry the current through a short connecting conduit to the transmission line magnets in a manner identical to the MS6 test string [51].

The power supply is actually two supplies in series. The main ramping supply generates the positive or negative voltage to transfer the inductive energy into and out of the magnets. It is not used when the magnet is at constant current. The second “holding” supply maintains the current during long periods at flat top and injection, and provides only the voltage necessary to overcome resistive losses in the current leads, warm buswork, superconducting splices, and the shorting SCR switch across the ramping supply. This approach minimizes the cost of the

ramping supply, simplifies the power distribution system, and moves the tightest regulation and ripple requirements to the precision holding supply.

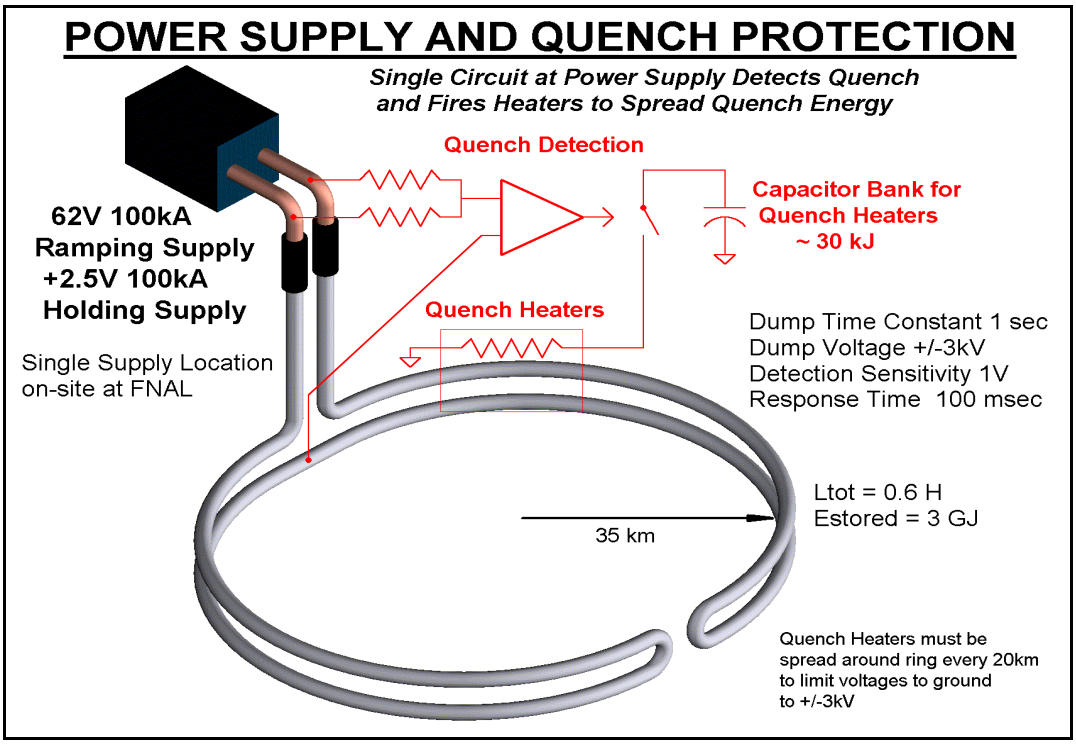

Figure 5.40. 100-kA power supply and quench protection for transmission line magnets.

The Main Ramping Supply design (Figure 5.41) is based on paralleling 8500 A modules of design similar to Main Injector supplies. This approach permits spare modules to be taken off line for repair, and allows the use of commercially available 10 kA DCCTs for current regulation. A 2-quadrant 12-phase SCR bridge returns inductive power to FNAL as the magnets ramp down. Ramping systems are designed to have rms power sized to be halfway between the peak (6.2 MVA) and the rms (3.1 MVA). This has proven to be a reliable design methodology for similar supplies at Fermilab. The rms feeder load of 4,800 KVA is less than one feeder cable for the source.

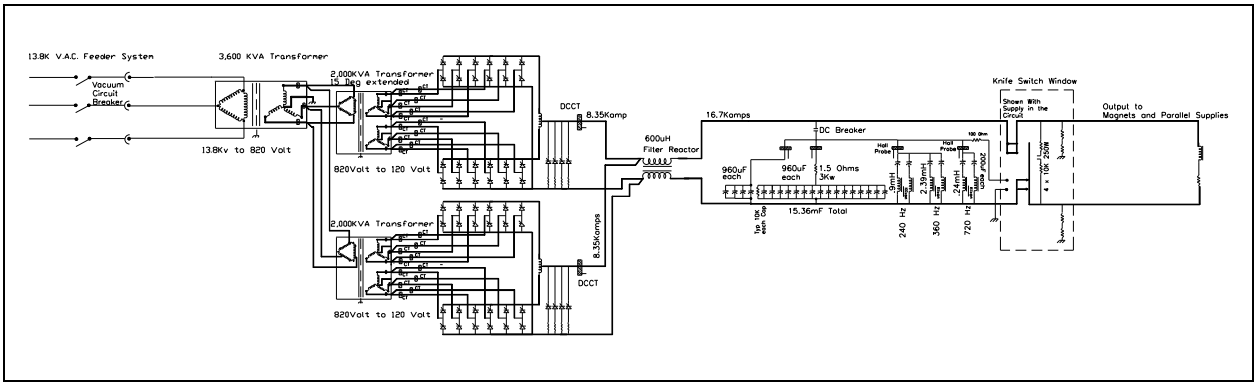

Figure 5.41. 100-kA ramping supply schematic (one 2 x 8.5-kA module shown).

The +2.5 V holding supply is essentially a copy of the 100 kA switching converter [52] constructed for the R&D magnet test. The device consists of a 450 VDC, 500 kW bulk supply followed by ten 10 kA DC-DC converter modules in parallel. This two-stage regulation scheme provides immunity to variations in input line voltage. The modules use IGBT chopper bridges, tape-wound cores and Schottky power diodes. The switching frequency is ~2 kHz. To minimize output ripple the 10 modules are phased to switch sequentially. This pushes the fundamental ripple frequency up to 10x the switching frequency or ~20 kHz. The switching will be phase locked to the revolution frequency so that beam emittance growth due to power supply ripple will be negligible. The control system for this switcher will be integrated into that of the main ramping supply to simplify regulation and load hand-off.

5.2.2.2 Current Leads

Superconducting current leads are required for both the main transmission line and for the IR quadrupoles. A single pair of 100 kA current leads is required for powering the transmission line. These could either be conventional copper leads identical to the leads developed for the MS6 transmission line test facility [51], or could be a specially built High-Temperature Superconductor (HTS) version using the 50 K transmission line shield flow as the inter-stage temperature. The cryogenic wall power associated with the conventional 100 kA leads is approximately 300 kW. This could be reduced by a factor of 4 with HTS leads [53]. Payback time for the electrical cost savings from HTS leads is approximately 3 years.

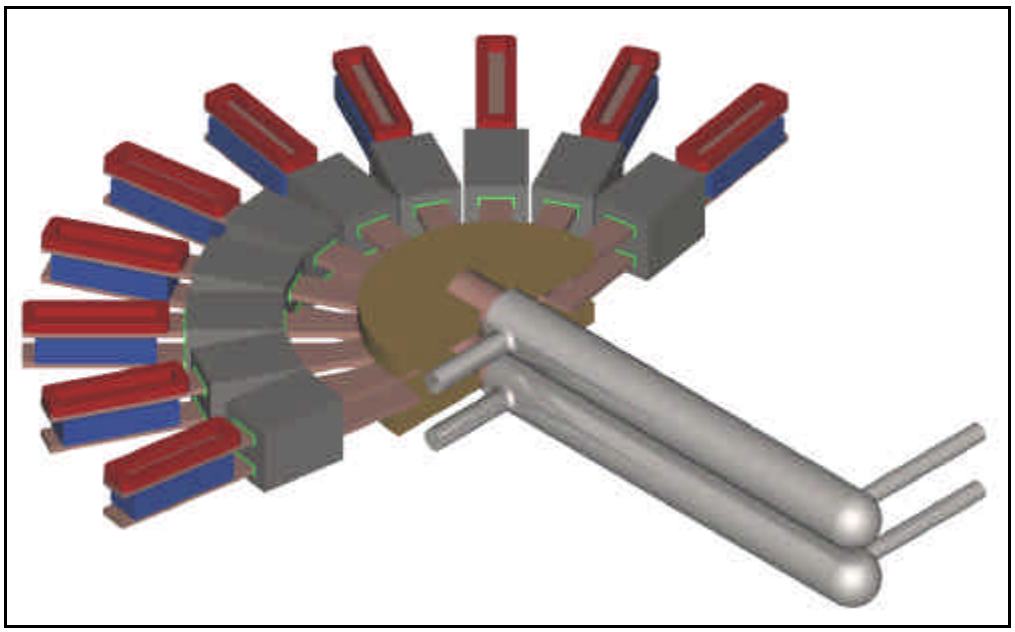

Figure 5.42. 100-kA superconducting current leads and switching converters developed for the MS6 test string. A more compact arrangement of the leads and power converter will be small enough to be placed in the tunnel and used for partial-ring commissioning.

IR quadrupoles can use commercially available HTS leads similar to the LHC. The total requirement for current leads in the Stage-1 machine is about 150 kA-pair, or about $1/12^{th}$ of the current leads required by the LHC.

5.2.2.3 Quench Protection

The only superconducting magnets of the Phase I collider are the transmission line magnets and the IR Quadrupoles. Protection of the IR quads with heaters is described in Section 5.1.4.

The low inductance and low stored energy of the transmission line magnet allows a simple and inexpensive quench protection system. The magnets themselves require no internal quench detection or protection circuitry. Ring-wide quench detection is performed by a single circuit located at the power supply terminals. Quenches are detected by a voltage imbalance at the power supply (Figure 5.40). When a quench is detected, magnetic energy is extracted with a 1-second L/R time constant by cryogenic "dump resistors" spaced at 20 km intervals around the ring. This keeps the peak temperature and pressure in the quenched section of the conductor at acceptable levels as described in Section 5.1.2.2. Quench protection system parameters are given in Table 5.23. The theory of operation is explained in [54] and a detailed write-up is given in [55].

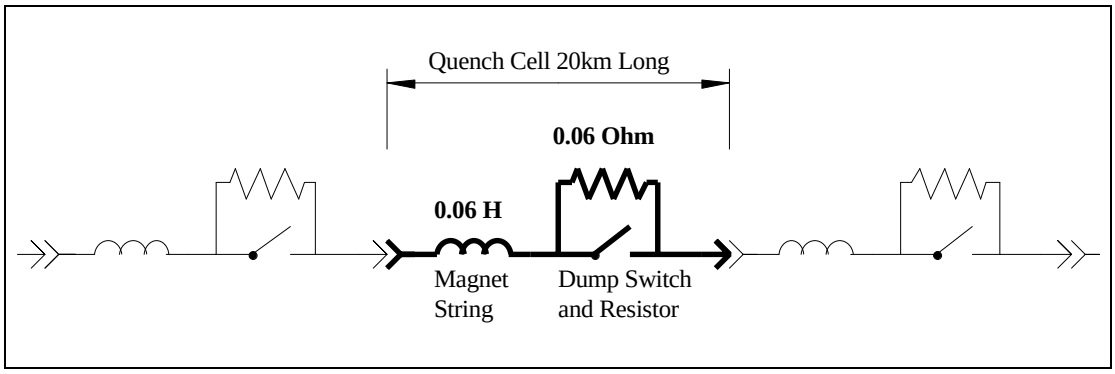

Figure 5.43. Quench protection cell of the transmission line magnet.

The "dump switches" are deliberately quenched sections of transmission line conductor built with Cu-Ni stabilized NbTi "switch wire"[56] which has a high normal state resistance. Current is transferred to a thick-walled Invar pipe that provides thermal mass. These dumps are efficiently recooled using helium from the cryogenic shield flows and transmission line flows, with the warm gas vented into the return header.

The protection circuit for the 100 kA current leads and power supply is integrated into the quench protection system. When an overtemperature or overvoltage is detected in the current leads, nearby copper buswork, or power supply components, the power supplies are shut off and a ring wide dump is forced. The required response time is equal to the thermal time constant of the leads or approximately 100 seconds.

It is instructive to compare this quench protection system to those of other accelerators. The LHC for example [57] requires a crate of quench detection electronics in the tunnel underneath each dipole in the tunnel. Each LHC magnet has more than 10 voltage taps and instrumentation feed-throughs. The LHC also requires a much larger array of energy dump resistors, dump switches, and current leads around the circumference of the ring. Despite the larger machine circumference, the quench protection system of the Stage-1 magnet is far simpler and should be more reliable.

Table 5.23. Stage-1 quench detection and protection parameters.

Transmission Line Current	100 kA
Magnetic Stored Energy @100 kA	10 kJ/meter, 2100 MJ/ring
Magnet Inductance at low field	3 μH/m 600 mH/ring
Energy Dump Time Constant	1 second
Peak Voltage To Ground during Dump	± 3 kV
I^2t during dump	5×10^9 A^2s
Peak Temperature of Conductor During Quench	250 K
Peak Pressure of Helium During Quench	35 Bar
Pressure relief during quench	Every 2 cells (500 m)
Effective Copper Cross Section of Conductor	3 cm^2
Quench Detection Threshold	1 Volt
Quench Detection Method (primary)	Analog bucking with midpoint of current return bus
Quench Detection Method (backup)	Deviation from V=LdI/dt at power supply terminals
Energy Dump Resistance	60 mΩ per location,
Dump Switch Locations	at cryoplants and midpoint of arc (20 km spacing)
Dump Switches	Quenched superconducting cables 65 m long
Superconducting Dump Switch Conductor	1:1 CuNi:NbTi “Switch Wire”
Cryogenic Dump Resistor Thermal Mass	65-m long, 3-cm ID, 5.5-cm OD Invar pipe
Final Dump Temperature after Dump from 100 kA	325 K
LHe Required for recovery after Dump from 100 kA	1600 liters (less if shield flow used for pre-cooling)

5.2.2.4 Straight Section (Warm Magnet) Power Supplies

The straight sections use warm iron/copper quadrupoles and a small number of other magnets. In each straight section all F and D quadrupoles are powered in series by a single supply. The IR straight sections have a larger number of independently programmable “tuning quads” but the total power and LCW usage is approximately the same as a normal straight section. The power supplies are located in shielded rooms (one per straight section) which contain ~500 kW of power supplies and are accessible with beam on. These are single quadrant supplies. Given the limited scope of these supplies it is desirable to make them fully redundant, especially those at the far side of the ring from FNAL. A detailed breakdown is given in [58].

Dipoles and quad correctors magnets identical to the arcs are provided at each quad location. Dipole magnets used to separate and cross over the beams are powered by the 100 kA transmission line and require no separate supplies.

5.2.2.5 Water Cooling (LCW) System

The “on-site” and “far side” straight sections require LCW systems. No LCW system exists in the arcs. Major heat loads are the resistive magnets, power supplies, and the RF klystrons. Loads are detailed in [58] and summarized in Table 5.24. The overall scope of the onsite LCW system is comparable to the MI-60 LCW system of the Fermilab Main Injector. The far site LCW system is about half that size.

Table 5.24. LCW and power dissipation summary for Stage-1.

	Heat Load	Total Loads	Total kW	LCW Flow (l/min)
On-Site Straight Sections	Resistive Magnets	188	4480	3200
	Power Supply Cooling	22	500	600
	RF Klystrons	16	3760	6400
	RF Loads & Recirculators	16	5600	4500
	Beam Stop	1	500	600
	Total (on-site)	227	14840	15300
Far Side Straight Sections	Resistive Magnets	176	3320	3500
	Power Supply Cooling	9	550	600
	Beam Collimation	-	40	50
	Total (far side)	185	3910	4150
	LCW Systems Total		**18750**	**19150**

The layout of the LCW system is sketched in Figure 5.44. The on-site straight section is connected to the Main Ring LCW system and can use the FNAL infrastructure for filling and makeup. Existing (unused) Main Ring ponds exceed requirements for power dissipation. New ponds and purification systems are required at the far side sites. The vertical drop generates a 150 psi pressure head, which is overcome by locating the circulation pumps at tunnel elevation and pumping the return flow upwards. The beam stop and beam collimation cooling systems require separate pumped loops for radioactive water (RAW) which will be heat exchanged with the main cooling water flow to maintain isolation.

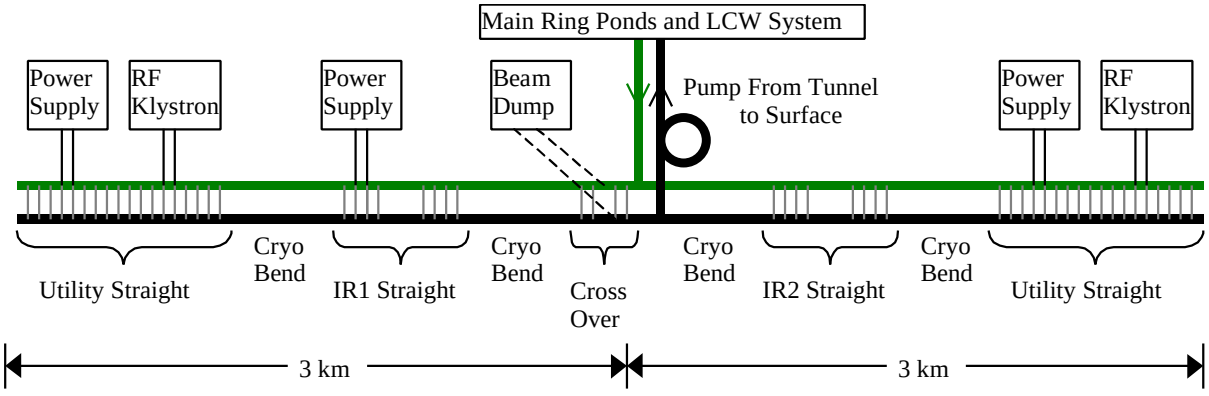

Figure 5.44. LCW system layout for on-site straight section. The far side LCW system is similar except that the RF loads are absent, the beam dump load is replaced by the smaller load from the beam collimation system, and an independent system of ponds and makeup water is needed.

5.2.3 Arc Instrumentation and Power Distribution

5.2.3.1 Reliability and Maintenance Considerations in the Arcs

The long arcs of bending magnets have specialized and limited requirements. The once-per-turn subsystems and their cabling, power and cooling requirements are absent. No LCW system is required. Only the repetitive instrumentation and corrector power supplies at each of the 1760 “half-cell locations” (every 135 m around the ring at the location of beta-max in each half-cell) are required. Infrastructure for power and communications occurs at alcoves at 10 km intervals.

Reliability is at a premium for the arc instrumentation due to the large size of the machine. Repair technicians at a centrally located facility require a 20 mile drive to reach the surface facility and begin access into the tunnel. Travel time will not be small compared to the 1.5 hour time needed to refill the machine and reaccelerate the beams. For this reason fully redundant capability is provided for all mission-critical subsystems in the arcs. Power distribution is provided to each module by two independent loop feeders with auto-resetting circuit breakers and remote disconnects. Two independent power supplies are provided for each corrector magnet and control function. Redundant network connections to each module are provided. The critical function of beam loss monitoring is provided by redundant sensors read out from alternate quadrupoles modules. The system design is such that even the failure of a handful of local electronics modules will not require immediate maintenance.

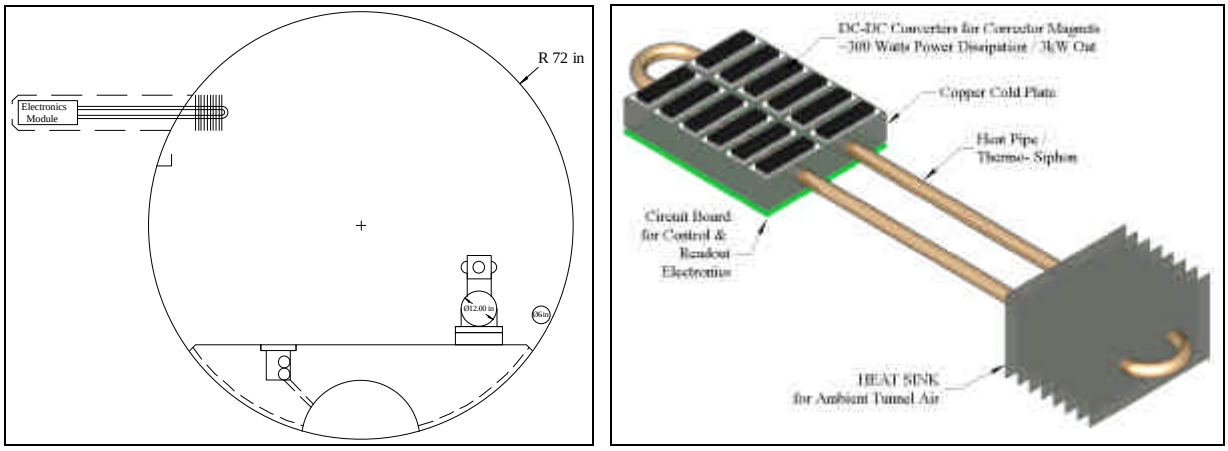

Figure 5.45. Electronics module at each quad location (every 135 m) contains beam instrumentation and DC-DC power converters for corrector supplies. Modules are in a radiation-shielded “hole in the wall” and dissipate their power in the ambient tunnel air via a heat pipe/thermosiphon and heat sink.

These electronics are located in a radiation-shielded modules buried in “holes-in-the-wall” at each quad location. All cables for instrumentation and corrector magnets are pre-assembled on the magnet and factory tested before installation. Cryogenic thermometry and a valve controller are used at every other quad location (270 m) to regulate the 50 K shield flow. Every 10 km there is a walk-in alcove associated with a tunnel egress point that contains conventional electronics racks and provides network connection, tunnel safety systems, bulk DC power for the instrumentation modules, and cryogenic instrumentation for the cooldown valve box. Average power dissipation is approximately 15 W per meter of tunnel, which can be air cooled.

5.2.3.2 Cabling in the Arcs

At the Fermilab Main Injector the cable tray to each service building contains 316 cables with a total cable cross sectional area of 180 cm^2 [59]. Over 95% of these cables service Beam Position Monitors (BPMs), Beam Loss Monitors (BLMs), ion pumps, corrector magnets, and temperature and vacuum monitoring. The superconducting Tevatron also has a large cable plant associated with quench protection and cryogenic monitoring and controls. The installation, termination, and testing of these cables are a significant cost and schedule item.

The Stage-1 design eliminates most cabling costs by multiplexing the signals to a local electronics module (Figure 5.45) at each half-cell boundary or "quad location." Signals are digitized locally and sent to the control room via network fiberoptics. Instrumentation and corrector magnets are clustered at the quad location and cable runs are typically 5 meters. Cable harnesses are prefabricated by outside vendors and mounted on the magnets and tested in the factory.

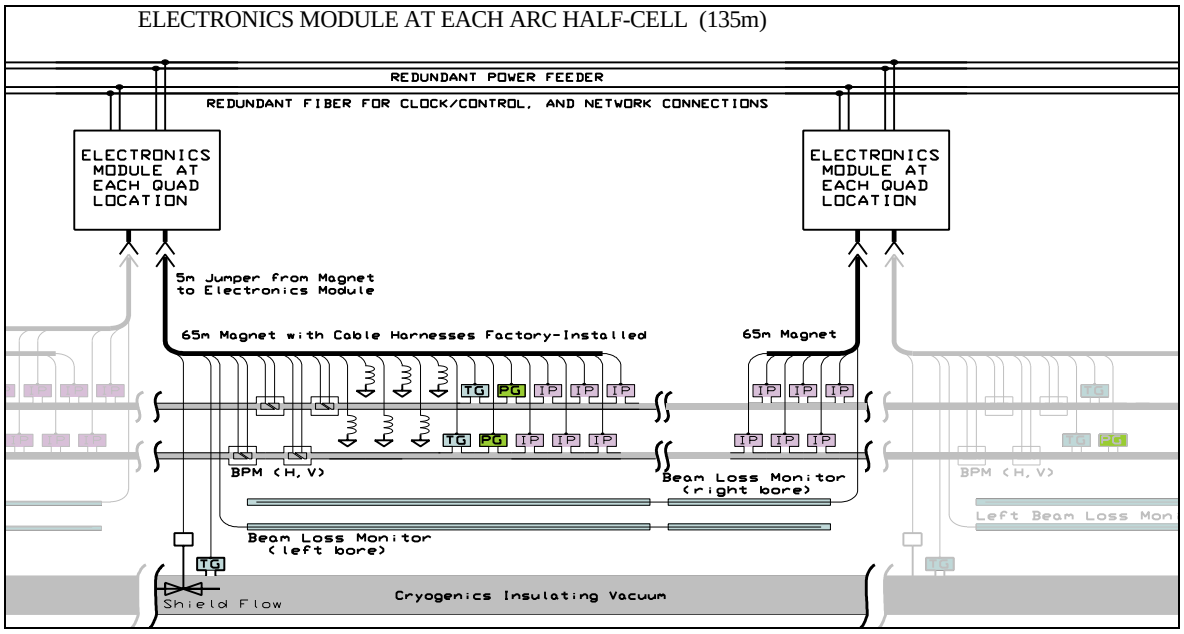

Figure 5.46. Cabling layout on the transmission line magnet. Cables and instrumentation are preinstalled and factory-tested on the 65-m magnets. Each magnet has a 5-m "extension cord" which jumpers to an electronics module located in a hole in the wall at each half-cell location (135-m spacing).

5.2.3.3 Corrector Power Supplies

The warm (air-cooled copper) correction magnets (Sec. 5.1.3) dominate the power consumption in the arcs. The electronics module at each quad location has 6-8 corrector magnet loads with a maximum installed power of approximately 1400 W. Average corrector power is < 1000 W in a realistic operating scenario. At maximum current approximately 90% of the power is dissipated in the magnets themselves with the remaining 10% (~150 W) in the power supply converters. Instrumentation and control power at each quad location is estimated to be ~100 W for a total of 250 W dissipated in the module. Power at this level can be passively

carried away from the electronics (Figure 5.45) via a heat pipe [60] and removed by the tunnel airflow of ~1 m/sec.

5.2.3.4 Power Distribution in the Arcs

Redundant DC-DC power converters are provided both for module control power and for each trim magnet. Power can be drawn from either of two redundant 1 kV DC feeders that loop the ring (see Figure 5.47). Power supplies are connected in parallel at each load. Under normal circumstances the load is shared and each power supply operates at < 50% of rated load, encouraging long lifetimes. Under failure conditions the load is taken over by a single supply which operates near its design rating (or less, if the corrector magnet setting is below 100%).

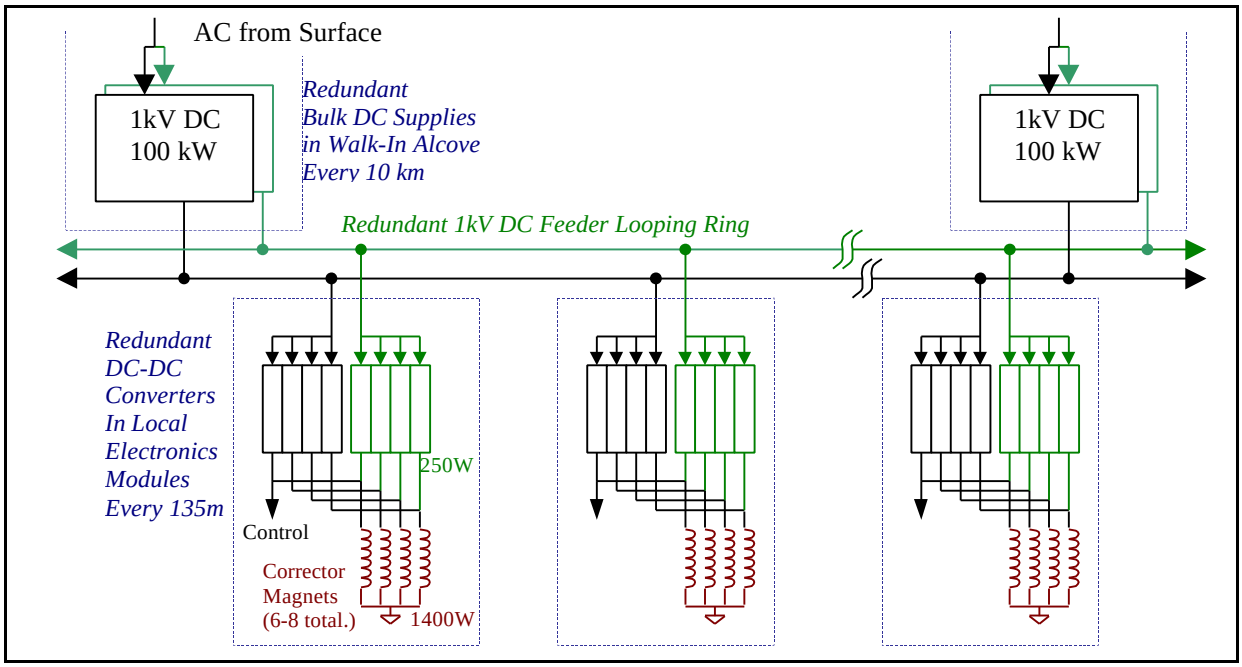

Figure 5.47. DC power distribution scheme in arcs. Redundant bulk DC supplies in walk-in alcoves every 10 km supply a redundant loop feeder. Each local electronics module contains two DC-DC converters for each load. Under normal conditions all supplies share loads and run at less than 50% of rated capacity. By means of auto-resetting circuit breakers (not shown), the system can tolerate short or open circuits on the loop feeders, a failure of one or both bulk supplies at any alcove, a failure of the AC surface feed to any single alcove, and individual failures on many corrector supplies.

Medium voltage 1 kV DC is chosen for power distribution to the electronics modules at each quad location. The DC is provided by 100 A bulk supplies every 10 km located in racks of electronics in walk-in alcoves. Two redundant bulk supplies are provided at each location, and two independent distribution loops are provided to route the power to the modules. Under normal conditions 25 A is sourced in either direction onto each of the 500 MCM loop feeders, and less than 3% of the power is lost in the distribution cabling. Under fault conditions one or both of the bulk supplies at one of the 10 km locations can fail, with the slack being taken up by adjacent supplies in the loop feeders. A short-circuit fault in one segment of the loop feeders can be tolerated by letting its circuit breaker trip and relying on the remaining loop feeder. Each

module is protected with fault current limiting via automatically resetting “solid-state fuses” [61].

The advantages of DC power in this application are as follows. The main power consumption is due to corrector power supplies that naturally operate as DC-DC converters. These are more compact than line-transformer based supplies, an important consideration for the local electronics modules. Modern DC-DC converters [62] have the following parameters: power density 200 W/in^3, efficiency ~90%, cost ~$0.35/watt. In fact, essentially all modern AC devices (e.g., fluorescent light ballasts, computers, high current welders, motor controllers) rectify the AC line power and then chop the signal using DC-DC techniques. Rectification at 60 Hz requires bulky capacitors and produces current spikes with power factor and noise problems that complicate AC distribution. DC power distribution makes the most efficient use of the copper in distribution cables, which is a major cost component in power distribution. DC power also simplifies the design of loop feeders, which may be powered from separate segments of the power grid without regard to the relative phase of the incoming AC power. Finally, by phase-locking the switching frequencies of the DC-DC converters to a frequency near the revolution frequency of the machine, the effects of power supply noise on emittance growth can be essentially eliminated as discussed in Section 5.2.2.1.

5.2.3.5 Beam Position Monitors (BPMs)

Both X and Y BPMs (Figure 5.48) will be provided every 135 m at the corrector region at each half-cell boundary (Figure 5.2). Although measurement of the second coordinate only improves the closed-orbit distortion by 10% [63], the added redundancy obtained by an independent readout of both coordinates will be beneficial given the small aperture and the travel distance to repair failed BPMs.

Button style beam pickups similar to those used on electron machines and the LHC are adequate. These devices are nonlinear outside the central 30% of their aperture. Given anticipated closed orbit distortions < 1 mm this is not a problem. In a few special locations near beam transfers where off-axis orbits must be measured, split-plate BPMs with better linearity will be used.

The BPM calibration offset can be verified *in situ* using the independently powered quadrupole correctors at each half-cell. The BPM can be accurately fiducialized to the warm iron of the corrector. At injection energy, the quad steering associated with a 1 mm orbit offset through the corrector generates an easily measured 3 mm orbit distortion as the corrector is powered.

BPM readouts using either AM/PM or Log Amp electronics are acceptable. In the case of Log-Amp readout both log(A/B) and log(A)+log(B) would be digitized to provide both position and intensity readout. In the case of AM/PM conversion a separate channel (possibly a log amp) is required to provide intensity information. In either case an in-situ calibration is desirable. The calibration circuit injects equal signals of adjustable amplitude into both channels to accurately determine the zero-offset response at different input strengths. A recent example of log-amp readout made for the SLAC B-factory fit on a 2.7” x 4.7” board that also included calibration circuitry [64].

Digitization bandwidth is determined by the first turn and transient response desired. A digitization rate >25 MHz can be supported by the DMA channels of today's Digital Signal Processors (DSPs), with no external components other than the flash ADC. A 10-bit digitization of log(A/B) would provide 20 μm least count resolution. Power dissipation for four channels of 10-bit 40 MHz digitization would be 300 mW total [65].

The cable run from the BPM to the local electronics module is about 5 m. This is long enough that the signal must be terminated but short enough that normal RG-58 can be used. The cable runs are short enough that no cable trimming for phase matching is required if AM/PM electronics are selected.

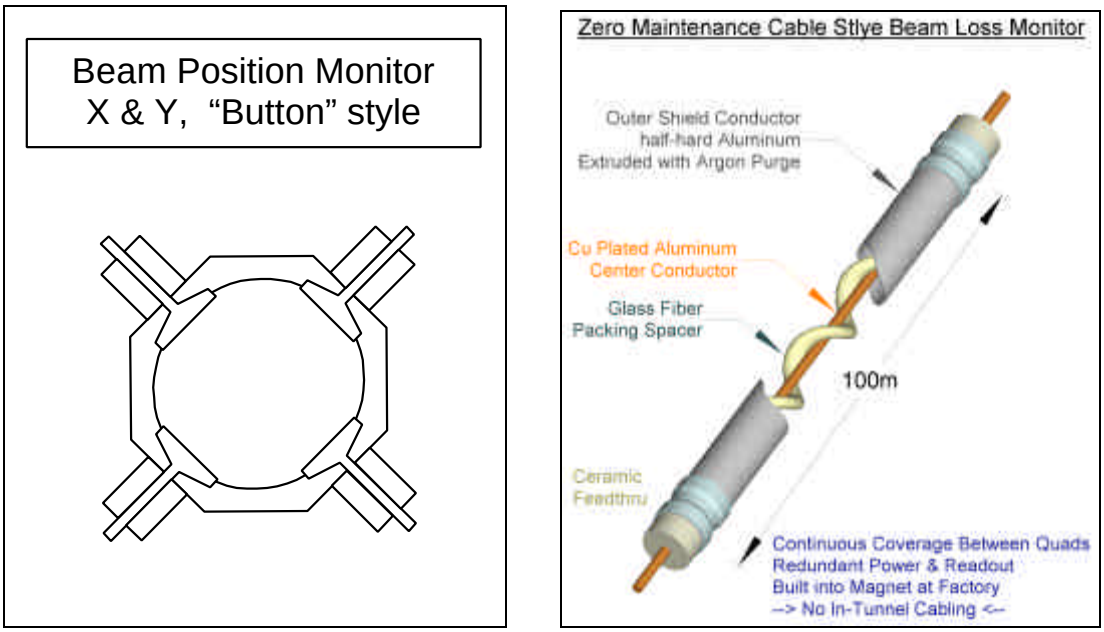

Figure 5.48. Beam Position Monitor (BPM) and Beam Loss Monitor (BLM) for Stage-1 magnets. The BPM is a capacitive "button" style typically found on small aperture beam pipes. The X and Y pickups are rotated by 45-degrees to avoid the synchrotron radiation (this is common at light sources). The BLM is a permanently sealed Argon filled cable-style ionization chamber. Two redundant BLMs run the full length of the magnet. It features all metal and ceramic construction similar to the Tevatron BLMs to allow the device to operate unattended for years (no gas bottle to change).

5.2.3.6 Beam Loss Monitors (BLMs)

The BLM function in the arcs is mission-critical in that no blind spots may exist which might allow chronic beam loss to go undetected. We therefore choose a cable style BLM. This is essentially a long ionization chamber that can provide complete coverage along the length of the magnet. The cable will be all metal/ceramic construction (Figure 5.48) so that no gas-bottle changing will be required. For redundancy, two independent cable BLMs are provided. Each runs the full length of the magnet but they are read out at alternate quad locations. This will provide complete BLM coverage even when the electronics module at a single location goes incommunicado. Separate BLMs on each side of the magnet provide some differential sensitivity to beam losses in each bore. Electronics required include a 2 kV/100 μA Cockroft-Walton DC-DC converter module, an op-amp integrator, and a medium bandwidth ~100 kHz 14-bit ADC. Power dissipation should be <2 W.

5.2.3.7 Ion Pump Power Supplies & Vacuum Gauges

Each 135 m half-cell contains 12 ion pumps (22.5 m pump spacing in each bore). These are powered and read out from the local electronics module. Each pump requires a 5 kV supply with a starting current of up to 30 mA but an operating current less than 0.1 mA. The power for all 12 pumps is provided by a single transformerless bulk supply (a 5-stage Cockroft-Walton converter operating from the 1 kV DC feeder). High voltage DC relays (Cotto 5501) isolate each pump and give the capability of providing the full starting current sequentially to each supply. Individual current readback on each pump is provided via an array of V/F converters operating at HV with an optically isolated data link to the DSP. Vacuum gauge readout for the beam and insulating vacuum will also be incorporated into the local electronics module.

Failure of the bulk supply shuts down all ion pumps in a 135-m half-cell. Pumping from the NEG strip remains intact. This results in a 50x rise in the pressure of a single gas species (CH_4) over the length of one half cell, equivalent to a 3% rise in the average pressure of CH_4 in the ring and < 1% drop in the overall beam lifetime. Redundancy in the ion pump power supplies is therefore unnecessary.

5.2.3.8 Network & Clock Connections

The electronics module at each quad location contains a DSP computer with an optical fiber connection running a network protocol stack. This CPU can store, average, spectrum analyze, and data-compress all digitized information before transmitting over a conventional fiber network. A separate dedicated fiber handles the FNAL-specific real time signals such as clock, event triggers, and beam abort heartbeat signals. These will be handled in hardware logic by a Programmable Logic Device (PLD) in the electronics module.

A minimal set of fiber connection to each module consists of one network connection plus one dedicated fiber for delivering Fermilab-specific signals. For cost estimation purpose we have assumed four direct point-to-point fiber connections between each quad location and redundant network hubs at located in the 10-km alcoves. The fiber cable will be a pre-assembled harness 5-km long with 4-fiber breakouts at quad locations every 135 m. Installation will consist of laying the fiber harness in the cable tray immediately below the electronics modules (Figure 5.49) and plugging the breakout into each electronics module.

The long-haul fiber backbone interconnecting the 10-km alcoves around the ring will be buried with the power duct in the invert. This provides additional radiation shielding to compensate for the longer distance of the backbone fiber runs (see Section 5.3.3.2).

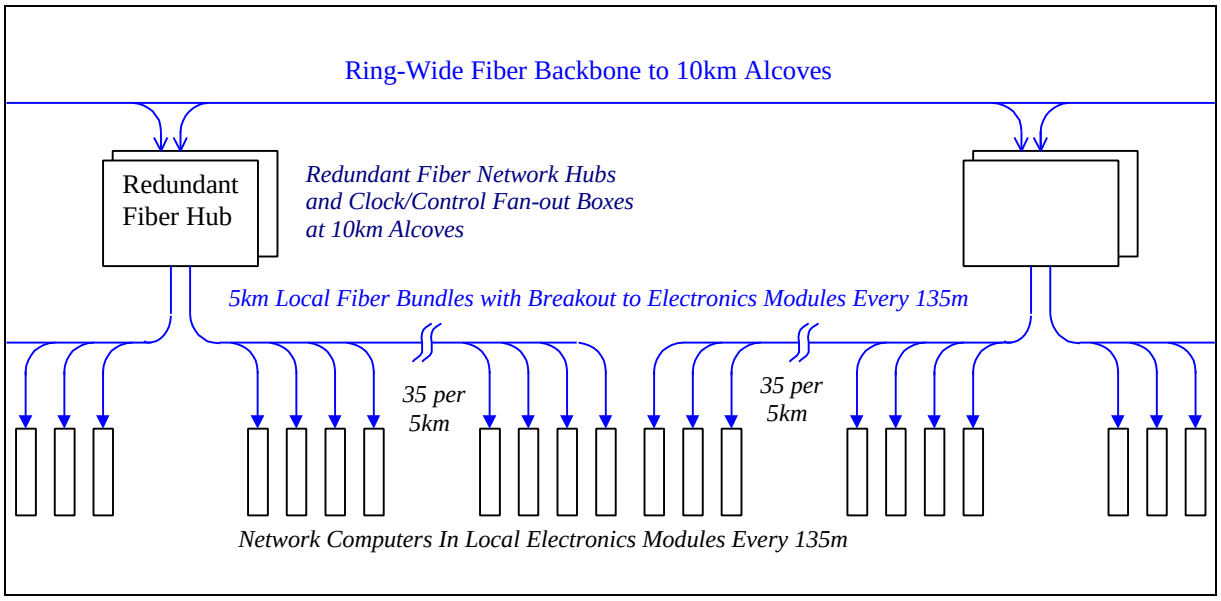

Figure 5.49. Fiberoptic clock and network connections in the tunnel, including redundant hubs and clock fanouts at 10-km alcoves.

5.2.3.9 Local Electronics Module Miscellaneous Functions

The networked CPU in each electronics module allows additional features to be added at relatively low cost. In many cases this requires adding only an interface IC, transducer and software to the local electronics module. The engineering effort for this is not unreasonable given the large quantity of local electronics modules. Some possibilities are:

- Tunnel temperature, humidity, and airflow transducers
- Integrated radiation dose monitor for the electronics module (FET + resistor)
- RF modules to communicate with the cell phones and PDAs of tunnel crews
- Microphones for detecting quenches and water problems
- Speakers to communicate with the above
- Cryogenic sensors and valve controls (presently estimated as a separate system)
- Vacuum valve controls (presently estimated as a separate system).

5.2.4 Beam Vacuum System

The beam vacuum system is divided into two sections. In the 225 km of transmission line magnets an extruded-aluminum warm vacuum system similar to LEP and electron storage rings is used. In the 8 km of straight sections synchrotron radiation is absent and the vacuum system will be a conventional stainless steel system similar to those commonly used at Fermilab.

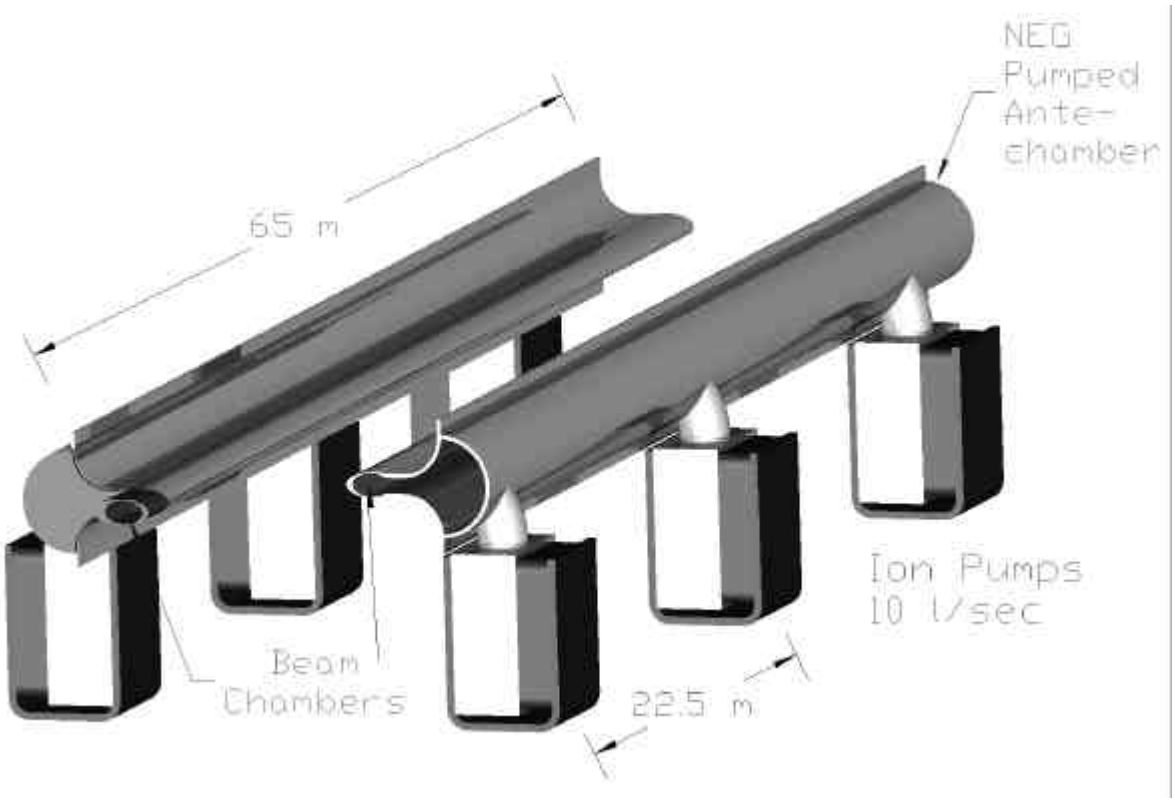

Figure 5.50. Extruded aluminum beam vacuum system in the transmission line magnets.

5.2.4.1 Arc Magnet Vacuum System

An extruded aluminum vacuum system (Figure 5.50) is used for the 225 km of arc magnets (450 km of beam pipe). The design of this system is driven by vacuum desorption from synchrotron radiation, the small aperture of the magnet gap, beam impedance and cost. Aluminum is chosen for reasons of economy and beam impedance. The system is pumped by a non-evaporable getter (NEG) strip located in an antechamber of the extrusion. Methane and noble gasses are pumped by 10 l/s sputter-ion pumps spaced every 22.5 m. The antechamber dimensions are chosen to provide adequate vacuum conductance to transport synchrotron-desorbed methane to the ion pumps. Pump power and vacuum gauges are discussed in 5.2.3.7.

The parameters and performance of this system have been analyzed in [66,67]. Inputs to the calculation included: 1) the measured synchrotron-induced desorption of major gas species from aluminum [68] as a function of the integrated dose of E_{CRIT} = 86 MeV photons, 2) the measured pumping speeds for NEG strip as a function of absorbed gas [69], 3) calculated conductances of the extrusion antechamber, 4) ion pump speeds for methane, and 5) scattering cross sections for the relevant gas species. This approach has given good agreement with the measured performance of LEP [70]. The result of the calculation (Figure 5.51) is that a beam lifetime greater than 200 hours will be achieved after approximately one week of operation. During the “beam cleaning” period the beam current will be increased from an initial 50 mA to the design value of 190 mA in five successive fills. The beam power scattered into the cryogenic system (Section 5.3.3) will not be a limiting factor during this time period.

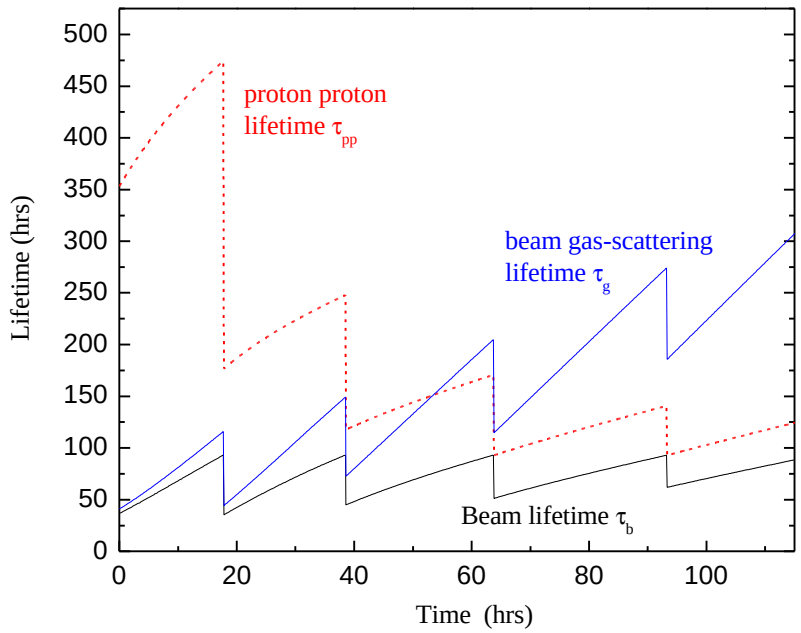

Figure 5.51. Beam scrubbing scenario for Stage-1 aluminum vacuum chamber. During the first 5 fills the beam current is increased from 50 mA to the design value of 190 mA. As synchrotron radiation desorption cleans the walls of the beam chamber, the vacuum lifetime increases to >200 hours.

Production of the aluminum vacuum system will be integrated into the magnet factory. Tunnel labor is minimized by pre-assembling 65 m lengths of extruded pipe which are installed in the magnets, cabled, and tested at the factory. Beam pipe extrusions 12 m in length will be received, inspected, and cleaned using an environmentally safe alkaline cleaning procedure developed at the APS at Argonne and used on the Fermilab Recycler [71]. The sections will be welded together to form 65 m lengths that include the Ion Pumps, NEG strips, feed-throughs and end transition sections. The assembly will be sealed, pumped and baked at 200°C for 12 hours in a 65 m long vacuum oven similar to the one built for the Recycler beam pipes.

The vacuum pipe assembly is then snapped into the C-magnet gap (Figure 5.52) in such a way that the beam chamber is pre-loaded against the magnet laminations. The preload prevents any possible loss of vertical aperture inside the magnet. The beam pipe has to be deformed slightly to get it inside of the horizontally focussing gradient magnet. This has been analyzed [72] in ANSYS and stresses are acceptable even for annealed aluminum.

The design does not provide for an in-situ bakeout. After factory bakeout the magnets will be stored and transported with the beam pipes capped off and under vacuum, and the beam pipes will be let up to dry nitrogen and the caps cut off to make the field joints in the tunnel. Under these circumstances an in-situ bakeout gains about a factor of 2 in initial dynamic outgassing [73], and gains very little after the beam scrubbing has completed [74]. A similar conclusion has been reached at the ELETTRA light source [75]. Our R&D program should verify this.

5.2.4.2 Straight Section Vacuum System

Synchrotron radiation is absent or reduced in most of the 8 km of straight sections and the vacuum system will be a conventional baked stainless steel / ion pump system similar to those commonly used at Fermilab. The 10 cm aperture of the 135 m stainless steel pipes between quadrupole locations is large enough that the beam impedance, alignment, and vacuum conductance are not a problem. The reduced apertures at the quadrupoles and corrector locations will be handled with 30 cm funnel transitions, which may be copper-plated stainless, or aluminum.

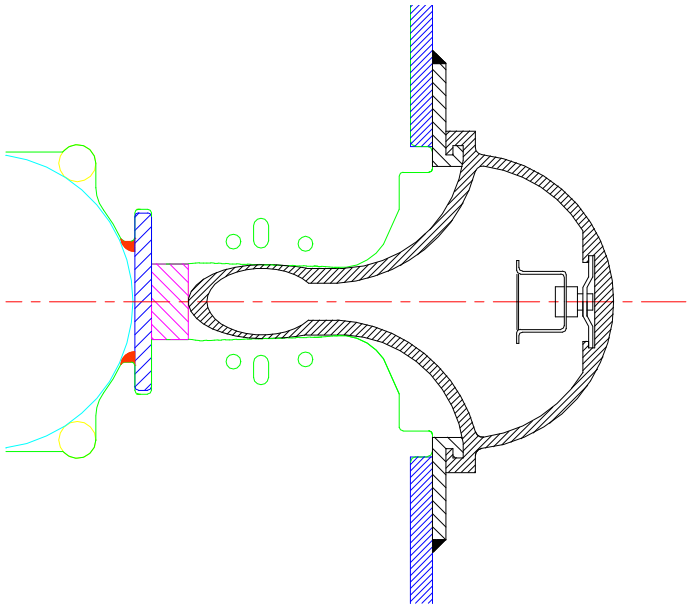

Figure 5.52. Cross section of beam pipe extrusion inserted into the magnet. During insertion the beam pipe is elastically deformed to fit it into the gradient magnet.

5.2.5 Once-per-Turn Instrumentation

A number of standard instrumentation systems occur only once per ring. In general these can be copied from existing systems in the Tevatron and/or Main Injector. The 53 MHz bunch structure and modest beam currents (~1/3 of Tevatron fixed target) provide no special challenges. Readout electronics for these systems is located in shielded rooms at the Utility Straight Sections. A warm beam pipe is used everywhere except at the IR triplet and superconducting RF cavities, so the instrumentation interface is simple. Physical layout of these systems is not heavily constrained since quadrupole spacing is typically 150 m, the beam pipes are separated by ~45 cm for much of the utility straight sections, and the transmission line and current return have been moved away from the beam to reduce fringe field. These are discussed more fully in [76].

Table 5.25. Once-per-turn instrumentation parameters.

FUNCTION	Occurrences	Readout Frequency	Comments
Tune Measurement	a few/ring	10 Hz	Use Arc Module DSPs for FFT?
Beam Current Toroids	1/ring		Also on injection lines
Sampled Bunch Display	1/ring	1 Hz	
Fast Bunch Integrator	1/ring	1 Hz	
Synchrotron Light Monitor	1/ring	1 Hz	
Ion Profile Monitor	2/ring	.1 Hz	Small beam size may be challenging
Flying Wires	1/ring	~few per store	

5.2.6 Radio Frequency Systems

Either superconducting or warm copper cavities produce workable RF acceleration systems for the Stage-1 machine [77]. During the design study acceptable parameters and costs based on the B-factory RF systems were developed [78]. The system described here is based on superconducting RF (SCRF). The advantages of SCRF are a higher energy efficiency during the long periods at storage flattop, and more flexibility to produce RF overvoltage to control beam instabilities if this proves to be an advantage.

The RF system parameters and some RF relevant machine parameters are summarized in Table 5.26. The RF frequency is 371.7 MHz, the seventh harmonic of 53.1 MHz. Overall the VLHC RF system is similar to the LHC RF [79,80], but with somewhat relaxed requirements for higher-order mode damping due to lower total beam current. The superconducting cavities are manufactured using niobium on copper technology developed at CERN. As in the case of LHC, there will be separate RF systems for counter-rotating beams. The beam separation in LHC is 420 mm. If we just scale cryomodule dimensions with RF frequency, we get beam separation of 453 mm.

To minimize the effect of the transient beam loading, cavities with high stored energy are preferred. The LEPII RF system experience [81] and tests of LHC [80] and SOLEIL [82] cavities show that it is reasonable to expect operating gradients as high as 8 MV/m. For VLHC we chose a gradient of 7.75 MV/m (3.125 MV per cell). Sixteen single-cell superconducting cavities are needed for each beam in the Stage-1 machine and 64 cavities are needed for each beam in the Stage-2 machine. The low *R/Q* of the LHC cavity helps to increase its stored energy. Still, the large (10%) beam gap will produce a very strong periodic modulation of RF phase of 27° for Stage-1 and 10° for Stage-2. This modulation is larger than at the LHC. A special RF feedback loop around the amplifier-cavity system assisted by the programmed phase modulation *a la* LHC [83] will be necessary to suppress this effect.

Each cryomodule will accommodate four single-cell cavities with cell-to-cell distance of $3\lambda/2$. The overall length of the cryomodule is approximately 5.6 m. The static heat leak of the cryomodule is 60 W and the RF cavity wall losses are 55 W/cavity, which yields a total cryogenic load of 280 W per cryomodule. The overall cryogenic heat load (without losses in cryogen distribution system) is 2.24 kW for Stage-1 and 8.96 kW for Stage-2.

Due to the rather small RF power per cavity, we propose to use 500 kW klystrons with 2 cavities per klystron in Stage-1 and 8 cavities per klystron in Stage-2. The number of klystrons required is 16 for each stage. A 500 kW CW klystron was jointly developed and constructed

recently by CERN and SLAC for testing LHC cavities [84]. The klystron has a high efficiency of 68% and thus the required AC power is 735 kW to generate RF output power of 500 kW. Then the maximum total wall-plug AC power for klystrons is 11.76 MW total for both beams.

Table 5.26. Summary of RF system parameters.

	Stage-1		**Stage-2**	
	Acceleration	Storage	Acceleration	Storage
Beam current	190 mA		68.9 mA	
Beam energy	0.9 – 20 TeV	20 TeV	10 – 87.5 TeV	87.5 TeV
Acceleration time	1000 sec		2000 sec	
Acceleration per turn	14.8 MV		39.4 – 18.15 MV	
Acceleration power (both beams)	5.62 MW		4.134 MW	
Synch. rad. loss per turn		0.03 MeV		12.37 MeV
Total s.r. power (both beams)		13 kW		2.1 MW
Revolution frequency	1286.5 Hz			
Bunch length, rms	142 mm	66 mm	81.9 mm	33.7 mm
Synchrotron tune	0.00845	0.00179	.00280	.00189
Synchrotron frequency	10.87 Hz	2.30 Hz	3.60 Hz	2.43 Hz
Bunch frequency	53.1 MHz			
Number of buckets	41280			
Bunch spacing	5.646 m, 18.8 ns			
RF harmonic number	288960			
RF frequency (7×53.1)	371.7 MHz			
RF wavelength	80.65 cm			
RF voltage	50 MV	50 MV	50 MV	200 MV
Accelerating gradient	7.75 MV/m			
Voltage per cavity	3.125 MV			
R/Q	89 Ohm			
Q factor at 8 MV/m	2×10^9			
Number of cavities	32 (16+16)		128 (64+64)	
Cavities per cryostat	4			
RF cavity wall losses	55 W			
Cryostat static heat leak	60 W			
Total cryogenic heat load	2.24 kW		8.96 kW	
Beam power per cavity	176 kW	0.406 kW	42.4 kW peak	16.4 kW
Number of 500 kW klystrons	16 (8+8)		16 (8+8)	
Number of cavities per klystron	2		8	

The klystron collector cooling water flow of ≥ 400 l/min yields a total cooling water requirement of 6400 l/min. RF water loads will need an additional 4000 l/min (during beam deceleration only) and ferrite circulators will consume 480 l/min. Thus the total amount of de-ionized water required for the RF system is 10,880 l/min per ring.

To estimate the cost of Stage-1 cryomodules we will use the formula [85]

$$C = k \cdot (0.8)^{\log(L)} \sqrt{\frac{1300 MHz}{f[MHz]}} \cdot L$$

Here L is the active length of accelerating structure; k = 200 k$/m is the cost factor. As one can see, the cryomodule cost scales approximately linearly with total length of the RF structure. The total cost of cryomodules for Stage-1 is then equal to 4.2 M$. The RF chain cost (including klystrons, high voltage power supplies, low level electronics, and RF distribution) is $1/W and totals to 8 M$.

The VLHC RF system would greatly benefit from R&D on improving the technology of sputtering niobium on copper with the goal to decrease if not completely eliminate the phenomenon of the Q slope. Special efforts should be devoted to understanding the nature of this effect. Success of this R&D would allow an increase of the accelerating gradient without seriously increasing the cryogenic heat load. Also, an R&D program is required to develop RF controls for heavy beam loading. Careful analysis of transients during injection, acceleration and beam storing is necessary and may necessitate having an individual klystron for each cavity [80].

5.2.7 Beam Dampers

In the last 30 years high intensity storage rings have become absolutely dependent on beam damper circuits. The Tevatron in fixed-target mode, the Booster, and the LHC will not operate anywhere near design intensity without them. At synchrotron light sources and B-factories the beams are lost within milliseconds without dampers. It is thus not surprising that the VLHC requires damper circuits to reach design luminosity for both Stage-1 and Stage-2 operation. Fortunately this technology is well developed. One new element which does occur in the Stage-1 VLHC is the necessity to distribute the dampers for one type of instability (the coupled-bunch resistive-wall instability) around the large circumference of the ring. While this provides some level of redundancy (since the beam is stable even if one of the distributed circuits fails) it is a new element which will be described below. Other dampers are conventional.

5.2.7.1 Distributed Transverse Dampers for Resistive-Wall Stability

Growth of transverse motions of bunches in the LF ring will be suppressed with active feedback systems [86]. The strongest beam impedance arises from resistive-wall. At the frequency of the first lower-sideband coupled-bunch mode, which is (1-0.235)f_0 = 0.99 kHz, the transverse beam impedance is (7.84+1.27j)10^{10} ohm/meter. This causes an exponential growth rate of 2.53×10^3 per second for a fully filled machine. Prompt cancellation of this growth is provided by six localized feedback stations spaced around the ring circumference. At each station, radial and axial damping are the same, and for each there are two feedback systems displaced azimuthally by 270° in betatron phase to address both ‘sine’ and ‘cosine’ phases of the oscillation; this makes the damping tolerant of tune changes that might be desired.

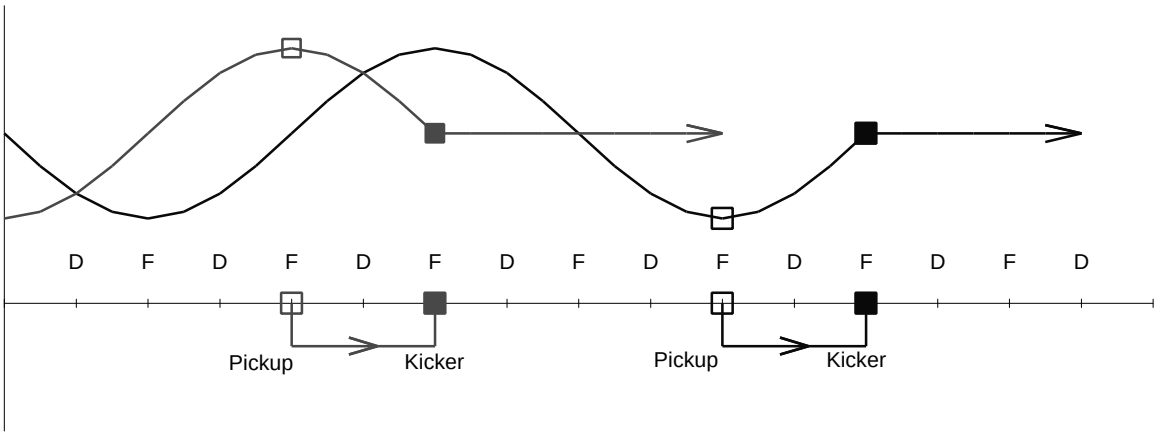

Figure 5.53. Layout of pickup and kicker positions for the horizontal coordinate at one station. Incoming beams with sine-like or cosine-like oscillations have their positions sensed by pickups at cell boundaries (F- locations) and are kicked back towards the design orbit after one-quarter betatron oscillation. An identical set of vertical pickups and kickers operates at D-locations. Six identical stations are distributed around the ring, one at each Stage-1 cryoplant location.

In localized feedback, a kicker is located downstream from the pickup by 90° in betatron phase (one lattice cell) and the signal is transmitted promptly from pickup to kicker through foam-insulated coax to minimize delay. Delay in the 271 meters of cable is 180 ns to which one adds about 50 ns for electronic processing and amplification. Although with this delay the signal from one bunch is delivered to the 12^{th} following bunch, the phase delay at 1 kHz is a negligible 1.5 milliradian. For higher-frequency sidebands the phase delay increases, becoming a significant 1/8-oscillation at 550 kHz. The localized feedback systems will be used up to 500 kHz; at that frequency the impedance has become small enough to be controlled by a conventional one-turn bunch-by-bunch system that extends up to the needed 26.5 MHz bandwidth of coupled-bunch modes.

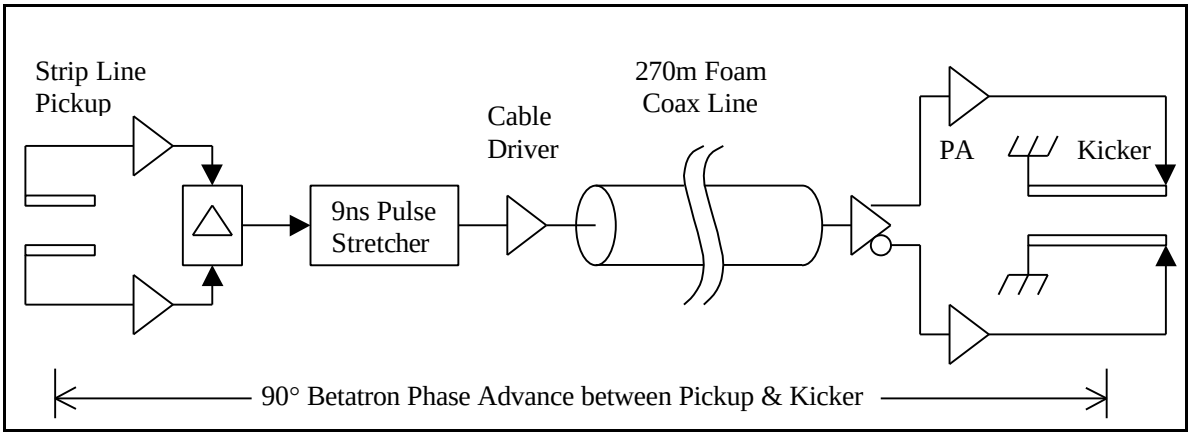

Figure 5.54. Electronic elements of the coupled-bunch feedback system.

The hardware in a local feedback system consists of (1) a pair of capacitive pickup plates, (2) electronics and cable to the kicker, and (3) a 4-meter long stripline-pair kicker. The pickup

strips are 25 cm long and connect to high-impedance amplifiers. The signals are then differenced and the unipolar pulses are stretched to half the interval between bunches to give a baseband signal for the kicker. At the lowest, strongest mode, the required feedback loop-gain is $G = 0.287$ and to damp injection errors of 0.1 mm calls for a transverse kick of 83.3 kV. The kicker delivers this with a power input of 1.10 kW. Injection in bunch trains separated by 2 seconds produces unwanted transients, especially if there is closed-orbit offset. Bunch signals will be recorded and analyzed to generate a correction for the local closed–orbit corrector; this will zero the closed-orbit well before the second train of bunches is injected. After the ring is filled, additional rejection of very low frequency excursions will be made by the low-frequency cutoff of the feedback electronics; this is possible with baseband operation as we have used here. For damping both radial and axial motions at 6 stations, 24 systems are required for each circulating beam.

Pickup and kicker are located at points of maximum betatron amplitude in slightly modified standard arc cells. The modifications (Section 3.2.1.4) involve removing 5 m of magnet iron at the boundaries of 8 successive half-cells. An additional quadrupole corrector is used at each location to repair damage to the β-functions caused by the missing focusing. The ~10% dispersion wave generated by the missing bend automatically cancels outside the insertion by virtue of the 360° phase advance across the 8 half-cells. The damper system uses at most 6 of the 8 available free spaces. Placing the damper pickups and kickers where the dispersion is nonzero is not believed to cause difficulties although this is will be the subject of continuing study.

At the coupled-bunch mode frequency of 500 kHz, the growth rate has been reduced to 57 per second or 0.044 per turn. This and all higher coupled-bunch modes are suppressed by the one-turn bunch-by-bunch feedback system that operates over the range 53.1 ±26.5 MHz. The kicker is a quarter-wavelength long at this frequency, 1.41 meter. The required kick for 0.1 mm excursion is 26.4 kV and power is 513 watt. Power amplifiers for this application are commercially available. The pickup is the same length as the kicker and feedback gain is 0.108. Radial and axial systems are similar.

One can ask if electronic noise in these dampers will add emittance during a long collision time. Fortunately, although the loop gains are high, the small aperture and peak bunch current of 8.4 ampere make the pickup signal strong and large electronic gain is not needed. The peak current gives a pickup sensitivity $IZ_L g / b\sqrt{2} = 2.6 \times 10^4$ volt/meter. Input thermal power with an amplifier noise figure of 1 dB is $1.2kTB = 5.2 \times 10^{-21} B$, where B is the bandwidth. Equating this to the pickup signal power with equivalent rms noise amplitude X_N gives $< X_N^{\,2} >= 3.7 \times 10^{-28} B$. The higher energy at collision reduces the gain to G =0.013. The 12 feedback systems would then cause an emittance growth rate, without allowing for damping, of

$$\frac{de}{dt} = 12 \frac{f_0 g}{2b} < G^2 X_N^{\,2} >= 2.1 \times 10^{-17} \text{ m/sec}$$

Since the nominal emittance is 1.7×10^{-6}, this dilution rate is of no concern. It would actually be smaller because of damping by the feedback. The broadband system produces a similarly negligible emittance growth.

5.3 Radiation, Machine Protection, and Beam Abort

5.3.1 Overview

The 2.8 GJ of kinetic beam energy in the Stage-1 machine is approximately eight times that of the LHC. Under normal circumstances roughly 50% of this energy is gradually dissipated in beam-beam collisions at the IRs. A few percent of the energy is lost diffusely due to beam-gas collisions around the ring, intercepted by beam collimation inserts which scrape away beam halo particles, and dissipated in the RF loads as the beam is decelerated. Somewhere between 40% (intentional beam abort at the end of the store at normal operation) and 100% (unintentional beam abort at certain circumstances) of the beam energy can be deposited in the external beam absorbers.

A very small fraction of the machine circumference exceeds the limit (~ 1 W/m of beam losses) for normal “hands-on” maintenance [87]. These regions include the small-angle regions of the IRs, the beam collimation system, and a small region of arc magnets downstream of the beam collimation system. The average radiation load in these components is a few times higher than the LHC, and the shielding and handling requirements comparable. LHC experience will be useful in optimizing these designs.

Under accidental conditions there is enough energy to cause severe damage to the magnet and surrounding environment. This is not a new situation for high energy colliders. The ISR beams had enough energy to repeatedly burn holes in the machine [88]. The magnitude of the problem has increased however. The beam of the Stage-1 machine carries enough energy that in principle it could liquefy 400 liters of stainless steel (whereas the LHC beam can only liquefy 50 liters).

Under worst-case accident assumptions the beam will leave the machine and strike the tunnel wall. We have begun to study the mechanical and radiological consequences. See Section 5.3.3. A single shot beam accident releases beam energy equivalent to losing the Main Injector beam at one place for about 4 hours. This is not outside the scope of existing shielding requirements at Fermilab, and should not be major problem for a tunnel in deep bedrock.

Tunnel groundwater activation from single-pulse accidents appears not to be a concern. A preliminary calculation indicates that it would be possible to lose the beam in a single spot, immediately transfer the activation into the tunnel water sump pit, and pump out the activated water without violating applicable Federal guidelines. Another way of saying this is that you could dump the beam into the tunnel sump cistern and the water would still be safe to drink. (This is of course a very pessimistic scenario, since in reality it will take days or weeks for the groundwater to collect in the sump, by which time most of the radioactivity will have vanished).

Effective strategies have evolved to deal with machine protection issues culminating with the Tevatron, SSC, and LHC. These issues have been revisited for VLHC energies [89,90] and the results are summarized here.

A robust and redundant extraction system removes the beam whenever the position becomes unstable or anomalous losses are detected. This protects the machine from anything that happens “slowly” (in milliseconds to seconds) such as magnet quenches, RF or power supply failures, vacuum failures or corrector magnet trips. Such a system has prevented the

Tevatron (so far) from having a hole burned through it. This is a standard feature, which continues to be essential at VLHC energies.

The one credible accident that occurs on a rapid time scale involves an abort kicker module misfire. The incompletely extracted beam will rattle around the machine and hit various well-defined limiting apertures such as extraction septa, IR quadrupoles, and beam collimators. The probability of this will be reduced in the LHC by replacing Thyratrons with solid-state kicker power supplies, and appropriate fail-safe logic which in principle prevents a single module misfiring. Since the probability of this cannot be reduced to zero, a set of "sacrificial collimators" are placed upstream of the vulnerable components. These are replaceable graphite structures that absorb and diffuse the beam energy. This strategy is essential at the SSC/LHC and will be necessary and sufficient for the VLHC.

Three qualitatively new features emerged while reviewing the machine protection situation at VLHC energies. First, the graphite core of the beam absorber may be damaged by a single pulse in the case of a sweeper magnet failure. The core must be protected (Section 5.3.2.2) with a replaceable sacrificial collimator immediately upstream. Secondly, in the case of a sweeper magnet failure the beam window in the extraction channel will have a hole melted in it. This is not a safety issue, but in this accident scenario the beam vacuum must protected with an automatically closing gate valve and the window(s) must be replaced. Finally, the beam collimation system (Section 5.2.3.4) will require water cooling for the jaws of the secondary collimators.

5.3.2 Beam Abort System

5.3.2.1 Extraction

It turns out to be quite straight forward to kick the beams out of the machine towards absorbers. The magnet parameters and layout are discussed in Section 5.1.5.4.2. Like the Tevatron, SSC and LHC abort systems, we use fast kicker magnets to switch the circulating beam into the other aperture of Lambertson magnets. The circulating beam goes through the field-free hole in the Lambertson magnets, and the extracted beam is bent upward in the Lambertson magnets so as to clear the first quadrupole in the downstream half of the straight section. A full aperture extraction kick is used and the separation of the circulating and extracted beams is 25 mm at the entrance to the Lambertson magnets. Thus any beam which is circulating anywhere in the physical aperture will be extracted. Special large-aperture warm-iron-and-copper quadrupoles are used near the Lambertsons so that no aperture restriction is presented to the circulating beam.

Normally the beam extraction is synchronized with an "abort gap" in the beam that has a length equal to the rise time of the extraction kicker. During certain control system failures it may be necessary to unconditionally extract the beam. This sweeps the beam across the extraction septum, which must survive without damage. For the VLHC the stress on the extraction septum is roughly equal to the LHC (since the beam energy per unit time is similar) and does no damage.

The requirements for the reliability of a one-turn extraction mechanism are comparable to the SSC [91] and LHC [92]. The extraction kicker is broken into 10 independent modules, with

any 7 out of 10 sufficient for a safe abort. Solid-state pulsers (as opposed to Thyratrons) will be used to minimize accidental prefires. Three Musketeer logic ("All-for-one, and one-for-all!") guarantees that any single module firing will automatically trigger the rest of the modules.

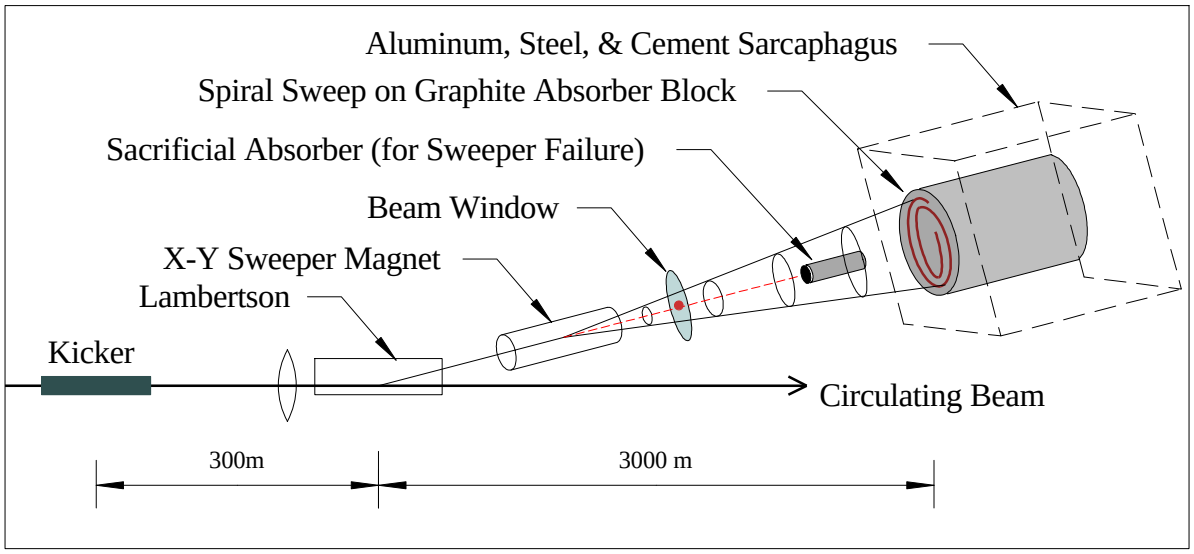

Figure 5.55. Schematic layout of beam abort channel including kickers, Lambertson septa, extraction beam sweeping, beam window, sacrificial rod, and graphite beam absorber. Under normal circumstances the extracted beam is swept in a spiral pattern to spread the energy across the graphite dump. If the sweeper magnet fails, the beam travels straight ahead into a sacrificial graphite rod, which takes the damage and must be replaced.

5.3.2.2 Beam Absorber

For TeV beams, the natural choice for the absorber is graphite, as at the Tevatron, SSC and LHC. The major difficulty lies in making the beams big enough that they will not crack a graphite absorber. A standard absorber consists of a graphite core, contained in an aluminum jacket with water cooling, followed by adequate steel and cement to protect ground water. The graphite core is rectangular, with dimensions 10 ×1.2 × 1.2 m. The thickness of steel shielding around the aluminum container is about 1.3 m on each side and extends about 3 m downstream. At present we consider a "4-in-1" design where extracted beams from both directions hit absorber cores in a common sarcophagus. The Stage-1 and Stage-2 machines share a common absorber for each direction.

Activation and cooling water considerations are driven by the average beam power on the target. The 300 kW average power (Section 7.4.1) corresponds to one full-energy abort of both beams every day and is equal to the 300 kW design value for the Main Injector beam absorber. The overall design is patterned on the Main Injector absorber that has proven satisfactory and meets ES&H requirements for this power level.

The graphite dimensions and beam size necessary to contain the showers without cracking the graphite were found by detailed simulations with the MARS14 code. The design goal was to keep the maximum temperature rise at the axis of the graphite core per spill below 1300-1500°C (from successful Tevatron dump experience and theoretical shock wave considerations). For a purely Gaussian beam with a spill that is stationary in transverse

position, the beam sigma would need to be 19 cm in both x and y for the maximum temperature rise in the core of 1330°C. Expanding the beams to this size with defocusing quadrupoles is out of the question.

5.3.2.3 Beam Sweeping System

A spiral beam sweeping scheme similar to the SSC and LHC is adopted to spread the beam energy across the absorber core. The magnets are described in Section 5.1.5.4.2. A horizontal and a vertical sweeper, 90° out of phase, both oscillate with decaying amplitudes. Ideally the frequency should increase as the radius of the spiral decreases in order to keep the temperature rise constant. Since this is electrically difficult, a suitable compromise is to limit the inner radius of the spiral to half that of the outer radius and accept a factor of two higher temperature rise at the inner radius. An estimate indicates that an outer radius of 30 cm would be adequate to keep the temperature below 1500 °C. If the beam sigma was 0.5 cm in both planes, the frequency of these sweepers would be 9.7 kHz.

In the case of a failure of both coordinates of the sweeper system the beam would damage the graphite absorber core [93]. To prevent this, a sacrificial graphite rod 5 cm in diameter and 4 m long is positioned on the beam axis immediately upstream of the main absorber. See Figure 5.55. Normally the extracted beams will spiral around this rod without hitting it. If the beam is extracted with all sweeping magnets off, the beam damage will be confined to the sacrificial rod. The rod will be housed in a metal box to prevent the spread of radioactive debris.

A beam window will not be protected in case of sweeping system (or defocusing quadrupole) failure, if the effective beam sigma on the window is less than 0.5 cm. The ring vacuum can be preserved by rapid-acting gate valves and/or multiple windows in series. Each window gets a small hole drilled in it when the sweepers fail, and pumping between the windows isolates ring vacuum until a slow gate valve closes. Alternatively, differential pumping with several wire meshes would do the same job. No personnel safety issues are involved.

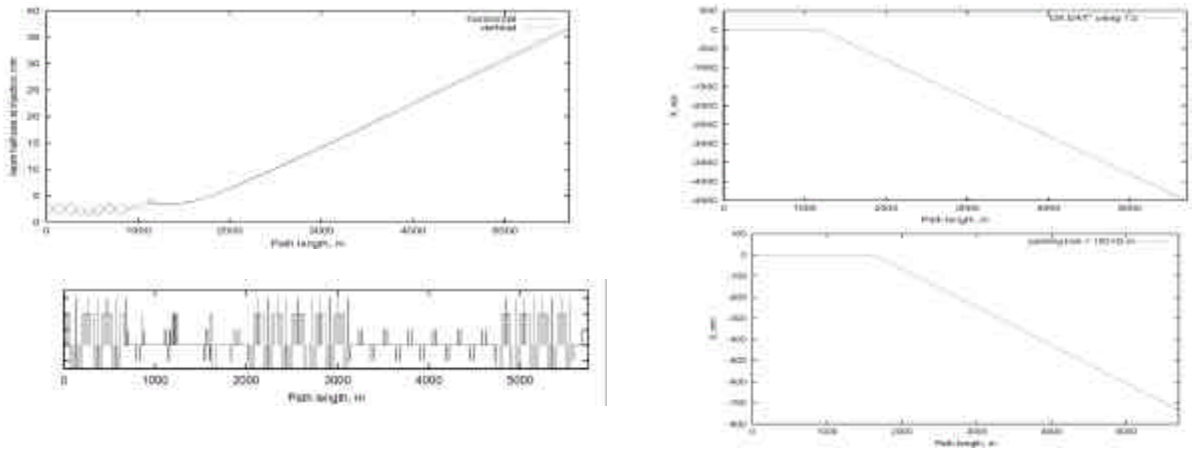

Figure 5.56. Beam sweeping system optics. Left: 3-sigma beam half-size at 1 TeV injection (beam size at 20 TeV is 4.5x smaller), and beam line layout. Right: beam displacement with respect to the direction of extraction straight section and maximum sweeping kick in the horizontal or vertical plane.

5.3.3 Radiation and Beam Loss

5.3.3.1 Quenches from Beam Loss in Transmission Line Magnets

The warm-iron design of the Transmission line magnet is less sensitive to radiation-induced quenches than ordinary superconducting magnets. To determine tolerable beam loss in the arcs, MARS14 simulations are done in the lattice both at injection (1 TeV, $\sigma_{x,y}$ = 1.4 mm, α_{inc} = 0.7 mrad) and top energy (20 TeV, $\sigma_{x,y}$ = 0.3 mm, α_{inc} =0.15 mrad). Corresponding materials and magnetic field distributions have been implemented into a 3-D model. Inward and outward beam losses were considered both for inner and outer beam pipes (see Figure 5.57).

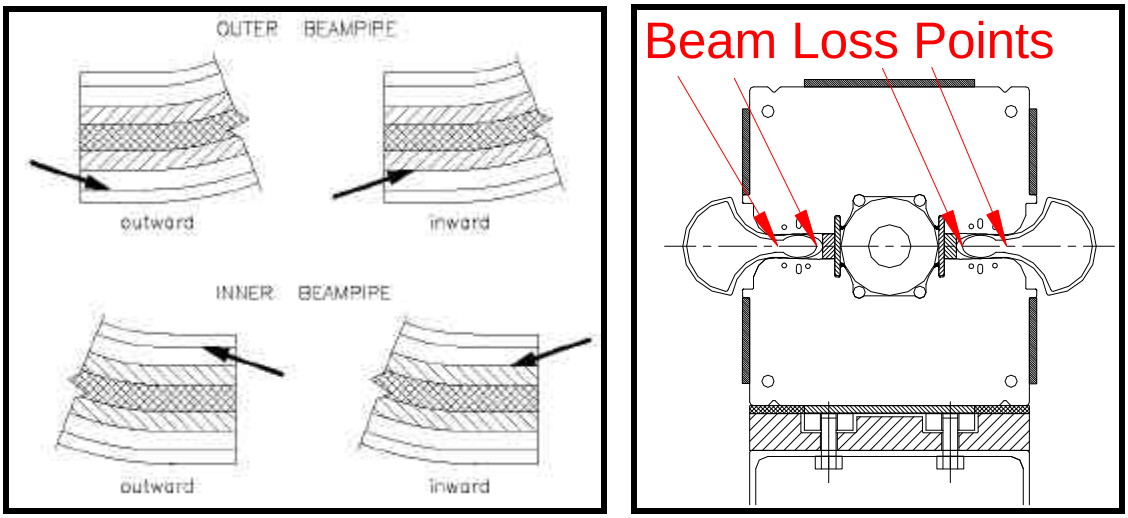

Figure 5.57. Beam loss geometries simulated in the Stage-1 VLHC magnets.

Simulations show that the superconductor in the transmission line magnets is rather well protected radially by warm iron. The energy deposition is diffuse and the peak temperature is relatively low at the hottest spot in the showers downstream of where the proton hits the beam pipe. Therefore, the tolerable beam loss is significantly higher than in a conventional cosine-theta type magnets. Table 5.27 shows fast (1 msec) and slow (0.1 sec) beam loss rates needed to initiate a SC magnet quench at injection and top energy in the Stage-1 ring. For comparison, the values for the Tevatron at 0.9 TeV are shown. This comparison assumes that the quench limits are the same in the VLHC conductor and the Tevatron dipoles. This assumption is probably pessimistic since the braided cable of the VLHC can re-route the current around a quenched region on the magnet midplane, whereas a cosine-theta magnet cannot.

Table 5.27. Quench-inducing loss thresholds (protons per pulse) for the Stage-1 VLHC and Tevatron.

	Fast Loss (ppp)	Slow Loss (ppp)
0.9 TeV	9×10^{8}	3×10^{9}
20 TeV	2.5×10^{7}	7.5×10^{7}
Tevatron	4×10^{7}	3×10^{8}

5.3.3.2 Cryogenic Heat Load from Beam Losses

Heat load from beam-beam interaction debris in the IR quads is included explicitly in the discussion in Section 5.2.1. The distributed heat load from beam losses in the arcs is also a potential concern. At 20 TeV roughly 5% of the energy from beam losses is estimated to be absorbed in the cryogenic transmission line. If 1% per hour of the (3+3) GJ of beam energy were lost uniformly in the arcs, this amounts to a total heat load of 800 W (3.5 mW/m average). This is a 5% perturbation on the 5 K heat load. The collimation system (Section 5.3.4) is expected to localize essentially all beam halo losses into collimators in warm sections, thereby eliminating that heat load from the cryo system.

The collimation system will be ineffective against losses from inelastic beam-gas scattering. With the expected vacuum lifetime (Section 5.2.4.1) of >200 hours, the cryogenic heat load will be < 2 mW/m, less than 3% of the 4.5 K heat load. If continued R&D reduces the 4.5 K heat leak this will become an increasingly important part of the total.

5.3.3.3 Radiation Damage to Tunnel Electronics

Section 5.2.3 describes electronics housed in small enclosures (“holes in the wall”) at each quad location. This approach was studied at UNK [94] and the electronics was found to survive under rather conservative assumptions about their radiation hardness. A recent interesting development [95] is that modern CMOS is found to be intrinsically rad-hard due to the absence of long-term charge trapping at the gate oxide layer in sub-micron devices. The LHC is apparently contemplating placing unshielded electronics under each dipole, and is initiating a study of the radiation hardness of commercially available electronics [96]. Depending on LHC operational experience, the rather modest costs of the module enclosures might be saved by eliminating the enclosures.

Radiation damage to fiber optics placed in the tunnel was studied at the SSC [97]. It was found that placing the fibers into the trough in the invert guaranteed their survival even for upgrades to 10x the SSC luminosity. We have followed this approach (Section 5.2.3.8).

5.3.4 Beam Collimation System

Even in good operational conditions, a finite fraction of the beam will leave the stable central area of the accelerator aperture because of intra-beam scattering, small-angle beam-gas interactions along the circumference, collisions in the IPs, RF noise, ground motion and resonances excited by the accelerator imperfections. These continuously generate a beam halo. As a result of beam halo interactions with limiting apertures, hadronic and electromagnetic showers initiated in accelerator and detector components will cause accelerator related background in the detectors, magnet heating and accelerator and environmental irradiation. The design strategy of the VLHC is that the beam losses are controlled as much as possible by localizing them in a dedicated beam collimation system. This minimizes losses in cryogenic parts of the accelerator, and drastically reduces the source term for radiation hazard analysis in the rest of the lattice. The technology for these systems has been well developed for the Tevatron, SSC, and LHC.

For the VLHC a complete beam cleaning system which provides for both betatron and momentum scraping has been designed and simulated [98,99]. The three-stage beam collimation system consists of 5 mm thick primary tungsten collimators placed at $7\sigma_{x,y}$ and 3 m long copper secondary collimators located in an optimal phase advance at $9.2\sigma_{x,y}$ and aligned parallel to the circulating beam envelope. Two more supplementary collimators are placed in the next long straight section to decrease particle losses in the low-ß quadrupoles and in the accelerator arc. They are located at $14\sigma_{x,y}$ to intercept only particles scattered out from the secondary collimators.

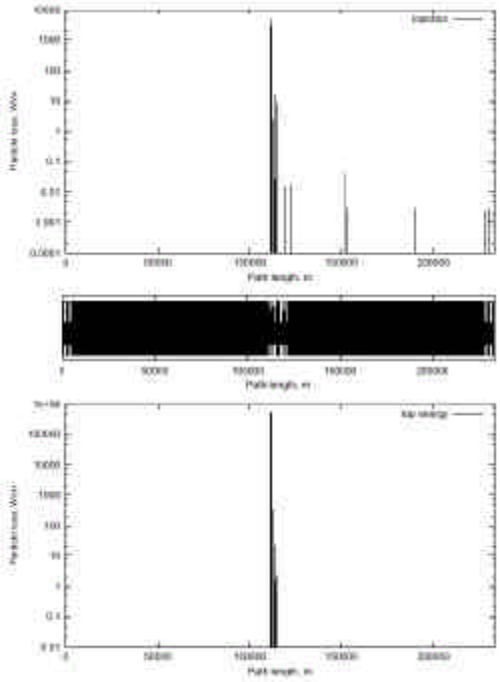

Figure 5.58. Beam loss distribution along the accelerator at injection (top) and at collisions (bottom).

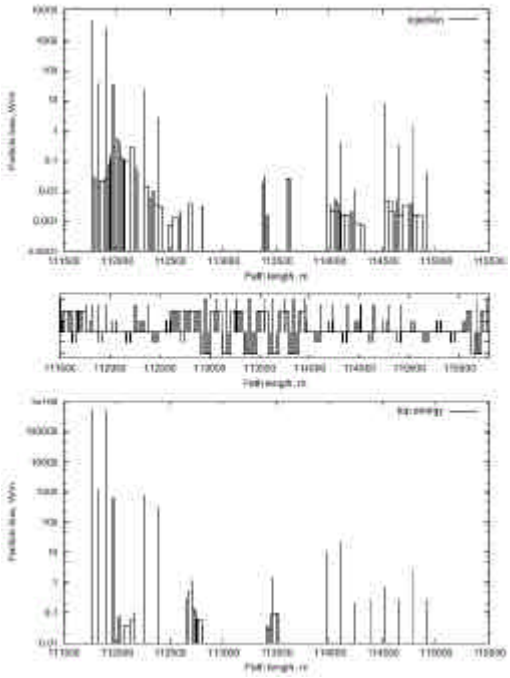

Figure 5.59. Beam loss distributions in the collimation section at injection (top) and at collisions (bottom).

Figure 5.58 shows that the simulated performance of the system meets the goal of essentially eliminating losses away from the cleaning insert. The main reason for this excellent performance is that the system uses a lattice insert specifically designed for this purpose, rather than something that has been retrofit into an existing machine such as the Tevatron. The maximum beam loss in the arc section behind the collimation region (Figure 5.59) is 1 W/m in two 21.5 m long dipoles and one 6 m long quadrupole, and 0 .2 W/m in two 21.9 m long gradient magnets.

The beam cleaning system was designed with the goal of reducing losses and detector backgrounds near the high luminosity insertions. Without the supplementary collimators, about 61 W of beam power (2×10^7 protons/sec) are lost upstream of the detectors. Including the supplementary collimators in our calculations, however, 6×10^4 particles are lost in the collimators, and we did not see any loses in the vicinity of interaction point. Further investigations should be done to determine ultimate particle backgrounds in the IP with the collimation system.

The primary collimation insert will be located in a far side straight section conjugate to the one of the on-site Utility Straight Sections. Secondary collimators will be located in this section as well as in special locations near the IRs. The secondary collimator will absorb approximately 20 kW of beam power and will require water cooling, probably thorough an isolated RAW (radioactive water) loop heat exchanged with the LCW flow. Shielding of the collimators will require approximately 1 m of radial iron followed by 50 cm of radial concrete over a length of ~15 m along the beam line to allow free passage of rad-trained personnel. This will require locally enlarging the tunnel cross section but should not require a bypass tunnel.

5.3.5 IR Protection

A sophisticated system must be designed to protect the IR SC magnets, particularly from kicker misfires. As in the LHC [100], it will consist of a front collimator, inner and intermediate absorbers in the inner triplet, and of a neutral beam dump and several collimators in the outer triplet. The similarity of the Stage-1 IR layout to the LHC makes it likely that a similar protection layout would be workable. The length of these sacrificial collimators will need to be increased due to the increased energy and decreased beam spot size of the VLHC beams.

5.3.6 Worst-Case Beam Accidents

Work has begun on understanding the implications of a “worst-case” beam accident in the VLHC. The assumption is that some unspecified agent causes the beam to be kicked out of the machine with a rise time fast compared to the revolution frequency, so that the normal beam abort does not have time to act. This agent is also assumed to possess a “kicker flat top” accurate enough (<1%) that the beam is effectively held in one place for the duration of the accident. Under these assumptions the beam will rapidly melt a hole in the magnet and impact the tunnel wall at near grazing incidence (3-5 mrad).

A preliminary observation is that the nearby cryogenic piping would rupture due to the rapid temperature rise. This would also be true of the Tevatron, HERA, and the LHC so it is important to keep this mysterious agent out of these machines as well. The cryo piping is contained inside carbon-steel structures (vacuum jackets and magnet iron) which would limit collateral damage. It would probably not even be noticed from the outside of the magnet. This is not our biggest problem.

A second observation is that the “beam drilling” scenario (in which a stable beam vaporizes a small channel deep into the target) is impossible at grazing incidence, even if the beam were perfectly extracted on a single trajectory. This beam drilling scenario is expected when the beam is normally incident onto a semi-infinite slab of material such as a beam absorber block. However at grazing incidence, the imbalance of the mechanical forces near the beam impact point (due to local heating of the rock) will cause a rock chip to “spall” out from the tunnel wall. This spalling behavior has been observed during rock excavation tests with electron beams [101] and follows this simple mechanical model. This spalling effectively sweeps the beam and guarantees that fresh (i.e. non-vaporized) material will be available to initiate the shower even if the beam is extracted perfectly. Thus the pattern of energy deposition can be calculated accurately enough by assuming that the shower initiates at a more-or-less fixed position near the point of grazing incidence.

A MARS calculation has been performed (Figure 5.60) to evaluate the energy deposition under the assumption that both the rock and beam position remain fixed. The simulation indicates that a region 8 meters long and about 15 cm in radius are heated to the melting point of dolomite. Obviously it will splatter to the floor. The next step in the calculation (in progress) is to use ANSYS to evaluate the thermal stresses in the surrounding rock and estimate the amount of rock that breaks off from thermal stress. The rise time of the heat pulse (1 machine revolution or about 0.8 msec) allows the mechanical stresses to relieve themselves on the scale of a couple of meters, so a static mechanical analysis is approximately valid.

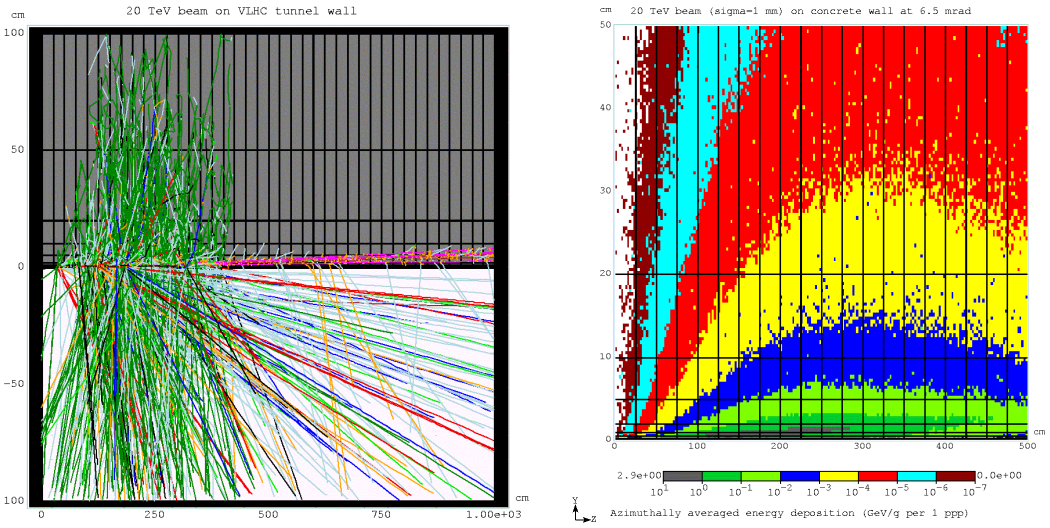

Figure 5.60. Stage-1 VLHC beam at 6.5 mrad grazing incidence on tunnel wall. The left picture shows particle tracks; the right picture is a map of energy deposition.

A more realistic situation in which the beam angle sweeps by even a few milliradians during extraction changes the situation significantly. In this case the heating is distributed into a large enough rock mass that the only a very small region (of order a centimeter wide) approaches the melting point. The picture becomes that of a destroyed magnet, a centimeter-wide scar on the tunnel wall, and an amount or residual radiation comparable to that of a 4-hour continuous beam loss at the Fermilab Main Injector.

5.3.7 General ES&H Considerations

5.3.7.1. Introduction

The VLHC with its two stages present a number of important considerations in the general area of environment, safety, and health. It is the intent of this section to identify the character of these challenges in a general way. Some of the considerations which must be taken into account are very similar to those that have been encountered and solved during the construction and operation of other facilities at Fermilab and at similar laboratories elsewhere in the United States and worldwide. Other novel issues have not been encountered on the same scale and require particular attention to assure their timely resolution in a manner that is cost-effective and that meets the approval of the public. In this section, both the conventional and the novel

issues are discussed. With adequate planning in the conceptual design stages, these problems can be adequately addressed in a manner that merits the support of the Laboratory, the Department of Energy, and the public.

5.3.7.2. Procedural/Regulatory Matters

The actual design, construction, and operation of the VLHC will have to meet a number of procedural/regulatory milestones to assure timely and continued support by the public and by the Department of Energy. ES&H requirements are currently set forth as a part of Fermilab's Work Smart Standards, incorporated in the contract between the Universities Research Association and DOE. Currently, the Work Smart Standards are reviewed annually to assure that they adequately address the hazards of the laboratory, including those of any new facility. If changes are necessary they are negotiated and the URA-DOE contract is revised accordingly. These standards include listings of applicable Federal and State Regulations as well as internally developed policies and national standards [102]. Of course, the contract under which Fermilab might operate in the future is likely to change in ways that could modify the applicable requirements.

A. Environmental Protection Procedural/Regulatory Matters

All DOE activities are subject to the requirements of DOE's regulations for implementing the National Environmental Policy Act (NEPA) [103]. A new project of this magnitude will be the subject of an Environmental Assessment (EA). A review will be done of all possible impacts of this project on the environment and the public. The required analysis is broad in scope and includes societal impacts along with those topics that are more generally associated with environmental protection such as the discharges of pollutants, effects upon wetlands and floodplains, and exposures of people to chemicals and radioactive materials. It will include a review of the alternatives of carrying out the project elsewhere or not at all. This process is centered on the production of a comprehensive document but also includes the participation of the public by methods that will be chosen by DOE. A likely result will conclude that that the preparation of an Environmental Impact Statement (EIS) is necessary since the VLHC extends far beyond the present boundary of the Fermilab site. The EIS process is generally considered to be an arduous one, but one that can be followed to a successful conclusion. The preparation of an EIS is certain to be a large task having significant cost, customarily accomplished using external resources. Regardless of the eventual path of the NEPA process, project funds cannot be issued to support a Congressional "line item" project beyond the early conceptual stage prior to the successful completion of the NEPA process. It is thus crucial that this process be conducted in a manner that is honest and which comprehensively addresses the potential concerns of members of the public. A good working relationship with the Department of Energy is also a necessity to a successful result.

Other procedural requirements apply in the area of environmental protection. These will be more certainly identified as a part of the NEPA process but early planning may well serve to avert problems later. DOE facilities are generally subject to Federal and State environmental protection regulations promulgated chiefly by the U. S. Environmental Protection Agency (USEPA) and the Illinois Environmental Protection Agency (IEPA). Some of the Federal and State permits apply during the construction stages, others apply during operations, and some apply during both stages. Permits are likely to be required to cover such topics as storm water

discharges, discharges of cooling water, wetlands mitigation, releases of air pollutants for both non-radioactive pollutants and for radionuclides, and construction in any floodplains. Archaeological sites might need further investigation and study prior to the commencement of construction. The preparation of the applications for these permits and approvals is generally straightforward. Early coordination with the project design team should greatly facilitate completion of the associated milestones. The VLHC is likely to be initially viewed by the public and by Federal and State regulators as a poorly understood, esoteric technology. In recognition of this and also because it will have an impact beyond the geographical boundaries of the present Fermilab site, early coordination with the Federal and State regulatory agencies is recommended as a vehicle to promote enhanced understanding of the nature and impact of the facility.

B. Safety and Health Procedural/Regulatory Matters

In accordance with Fermilab's Work Smart Standards, the Laboratory will be required to prepare an assessment of the ES&H issues associated with this project in the form of a Safety Assessment Document (SAD). Given the size, scope and cost of the VLHC, the preparation of a Preliminary Safety Assessment Document (PSAD) is needed. The purpose of the PSAD is to identify the relevant ES&H issues at an early stage and propose how they might be mitigated. A final Safety Assessment Document (SAD), then, documents the resolution of all the pertinent issues raised by the PSAD. Environmental issues are customarily integrated into the PSAD/SAD process to promote program cohesiveness. It is nearly certain that DOE will choose to review these safety documents by utilizing an external review team. Just prior to facility operation, a readiness review will be conducted in similar fashion using an external review team. Unlike NEPA assessment activities, PSAD/SAD activities generally begin after funds are issued. Nevertheless, careful consideration of PSAD/SAD in the design can only result in beneficial results. Efforts should be taken at early stages to promote consistency between the conclusions of the NEPA assessment and the safety and health documentation.

DOE is presently "self-regulating" in the areas of industrial safety and occupational radiation protection. There is a possibility that during the development of the next accelerator facility, DOE activities might become subject to "external" regulation in these areas, as well as in occupational radiation protection. It is difficult at this time to anticipate the form such external regulation might take or which agencies might be involved.

5.3.7.3. Occupational Safety During Construction

The VLHC requires a large amount of tunneling in bedrock units, most of it horizontal or nearly so, and other tunnels with slopes. In addition to the safety requirements pertaining to construction activities, Federal regulations pertaining to underground operations (e.g., "mining" activities) come into play. Solutions to these issues are being developed to address challenges of this type encountered in the excavation for the NuMI project. These include the standard concerns about tunneling safety and material movement as the tunneling proceeds. Tunnel Boring Machines (TBMs) will be used for most of the tunnel. For some portions of the underground facility the drill and blast method will most economical. Both methods have associated occupational safety considerations. Provisions for emergency response including underground rescues will be needed. Egress issues relevant to protection of the construction workers will be of paramount importance.

It is clear that stringent measures must be taken to prevent flooding both during the construction period and thereafter. This problem must be addressed in harmony with the related environmental protection concerns (see Section 5.3.7.4). Downward slopes in the bedrock units will require attention to the prevention of uncontrolled movements of heavy objects downhill. While such control measures are well within those encountered in mining operations elsewhere, they are novel at accelerator laboratories.

During project construction, industrial radiography, a tool commonly used in general industry, is likely to be employed to assure the quality of pipe welds. Such radiographic operations, which typically use radioactive sources of high activity and relatively hazardous compared with the sources commonly used in particle physics experiments, would need to be conducted in compliance with the pertinent requirements of the State of Illinois in order to control the hazard to personnel. In the course of construction, other radiation-generating devices such as soil density gauges and media water-content probes might also need to be used. Standard procedures pertaining to such activities should be applied.

5.3.7.4. Environmental Protection During the Construction

A small portion of the VLHC will be located near the surface, in the glacial till, while most of it will be located deep underground in various rock strata. For the portions near the surface, construction may proceed by cut and fill techniques similar to those employed to build most of the present facilities at Fermilab. Erosion control measures similar to those in practice for a number of years will be employed in accordance with good engineering practice and Federal and State regulations. Dust from any spoil piles must be kept under control. Likewise, a storm water management plan will need to be developed. Noise from construction activities is not expected to be significantly larger than that associated with normal civil construction activities in the vicinity of Fermilab. The NEPA process will result in a determination of the impact of the project on wetlands and or floodplains. It may be necessary for compensatory man-made wetlands to be created.

Tunneling in the bedrock units will result in the removal of a considerable volume of rock. The management of the spoil is a major issue that must be addressed and provisions for its proper stockpiling provided. In particular, concerns about dust may be more severe for this material, largely pulverized rock. The duration of this storage may be temporary for the spoil that is of marketable quality and longer for that reused at Fermilab or disposed. This should be carefully planned in accordance with Fermilab's longstanding tradition of placing high importance on aesthetic issues. The management of spoil materials will need especially vigorous attention off site. The placement of such a project in any aquifers results in the need to protect drinking water resources from contamination during construction. Also, the "de-watering" of tunnels, as the construction proceeds will require measures to prevent the depletion of wells and also to manage effectively any additional water discharges from this source.

The storm water management plan will need to take into account any releases of groundwater generated in the course of "de-watering" the tunnel. Careful hydrogeologic studies need to be performed to understand the interplay of the construction of the project with the various aquifers. This must be done to establish with certainty that the construction activities will not cause significant perturbations of the local individual and municipal water supplies.

The exact depth of the various aquifers is not known in detail at all locations and accurate measurements will be needed. The results can be used to plan a strategy for preventing the tunnel from serving as a possible path of cross-contamination from one aquifer to another. During construction activities, precautions are needed to guarantee that spills of chemicals, including lubricants and fuels from the construction equipment, are captured before they enter the groundwater.

Tunneling activities can generate considerable noise and vibration. For blasting techniques, quantitative standards apply to the amplitude of the vibrations that are allowable at the surface. Noise exposure, both occupational and to the public at the site boundary and at off site locations will be an issue that needs to be addressed.

5.3.7.5. Occupational Safety During the Operations

A. "Ordinary" Occupational Safety Hazards

In this section, the focus is on the issues that have been successfully addressed before, at Fermilab and elsewhere by well-known techniques.

- The facility will use high current electrical circuits on a large scale. Present techniques in managing power distribution and providing means to effectively lock out supplies should be adequate to address the electrical hazard.
- Radio-Frequency (RF) generation and distribution equipment will be used extensively. Present techniques for controlling possible exposures to non-ionizing radiation should be sufficient.
- Large amounts of cables, transformers and electrical switchgear will be installed underground. Current methods for addressing fire protection concerns should be adequate.
- Long tunnels will be present. There is a need to adequately address Life Safety Code/fire protection issues to assure adequate provisions for egress and adequate means of prevention of and response to fires.
- There will be movements and alignment of large, heavy components. There is a need to include considerations in the design related to ease of movement of equipment to facilitate the prevention of injuries.

B. Novel Occupational Safety Hazards

This section is directed to those occupational safety hazards that are not generally encountered at accelerator facilities. These will require consideration in the early planning stages in order to be addressed in an efficient manner.

- The VLHC requires the extensive use of superconducting materials and cryogens. While these technologies are relatively new, a number of accelerators worldwide have developed techniques adequate for addressing them. Provisions will need to be made for the safe release of cryogens to the surface both during normal operations and in the event of quenches. Current accelerator facilities have developed mechanisms for using skilled engineers to independently review such systems for safety during the design and commissioning stages. The result has been the development of a number of standard

engineering practices to mitigate both direct cryogenic hazards and the accompanying oxygen deficiency hazards (ODH).

- As during construction, the strong desire to minimize the number of exit points will render adequate design and engineering with respect to the Life Safety Code imperative. It is likely that special means of communication underground will need to be provided, "refuge" locations incorporated into the design, and adequate means of transport of personnel, both healthy and injured, to the surface established. These provisions will need to incorporate recommendations of a qualified fire protection professional at the time of the development of the conceptual design in order to assure adequate allowances for their costs. Later involvement of fire protection engineering will also be needed as the detailed design proceeds.

5.3.7.6. Ionizing Radiation Safety During Operations

A. Prompt Radiation Shielding

The siting of the VLHC deep underground will provide adequate passive shielding to attenuate prompt radiation to levels acceptable to the members of the public. The shielding of proton accelerators needs to attenuate the neutrons produced at large angles. At the forward angles, given the copious production of muons, and the increased importance of range-energy straggling at high energies [104], the shielding requirements must be well-understand at the earliest possible stage in the design and in the NEPA process.

Current Department of Energy requirements are not well matched to discussions of radiation fields that exist beyond the boundaries of DOE sites. DOE has specified the annual limits on the radiation dose equivalent that can be received by occupational workers and members of the public (see Regulation 10 CFR 835) [102,105]. These limits, in all situations expressed to date, pertain to the dose equivalent delivered to people or to locations where people could reasonably be. For individual members of the public, the primary limit is 100 mrem (1 mSv) in a year, not including man-made, medical, or enhanced natural radioactivity. Special reporting requirements apply when the annual dose equivalent received by an individual exceeds 10 mrem (0.1 mSv) in a year. DOE has expressed the view that non-occupational annual doses to members of the public are not expected to exceed a few mrem in a year. In light of public concerns about radiation exposures, any new facility should be designed to keep the dose that could be reasonably received by actual members of the public to as small a value as possible.

B. Residual Radioactivity of Components

In the high-energy region, most, but not all, of the radiation effects scale roughly with the beam power. In particular the effects of high residual activity levels should be carefully taken into account at early stages of design of beam cleaning and abort systems and other locations of possible high beam loss. Doses that might be received by workers are an important subject that must be assessed as a part of the NEPA process. The need to minimize the generation of radioactive wastes and to eliminate the creation of wastes that contain materials that are toxic or hazardous, and which contain radioactive waste, is an important concern.

C. Airborne Radioactivity

Federal Regulations promulgated by the USEPA have established an annual limit on dose equivalent of 10 mrem (100 μSv) to any member of the public that can be received as a result of operations of DOE facilities such as accelerators [106]. Further, the same regulations impose stringent continuous monitoring requirements if the annual dose equivalent to any member of the public is to exceed 0.1 mrem (1 μSv) in one year. In addition, if the level of 0.1 mrem in one year is to be exceeded, then an application for approval to construct and a notification of startup must both, in proper sequence, be submitted to the USEPA. Given the extent of the VLHC beyond the present boundaries of the Fermilab site, careful attention must be paid to the production of airborne radioactivity.

D. Radioactivity in Soil and Groundwater

The VLHC siting requires that the production of radioactivity in hydrogeologic units be given careful attention. Before the exact footprint of any chosen facility is irrevocably determined, detailed hydrogeologic studies should be conducted to determine the relevant parameters precisely, as they are known to vary significant in the vicinity of the Fermilab site. It is clear that protection of groundwater against contamination with radioactivity merits early, detailed attention in project design to assure satisfaction of likely public concerns. It may well be that the most prudent choice of design objectives might be far below present regulatory standards for drinking water.

5.3.7.7. Non-Radiological Environmental Protection Issues During Operations

Operations of the facility should be planned in a way that incorporates proper measures to control the generation of non-radioactive wastes. Further, there is a need to address potential spills of hazardous or toxic materials in a way that fully protects members of the public and of environmental resources. The detailed attention to these issues will be required as part of the NEPA process and the designs should provide information of the quality needed to support all required permit applications to State and Federal environmental regulatory agencies. In any enclosures located deep underground the cross-contamination of the various aquifers must be prevented and any de-watering operations must assure that local community or individual drinking water supplies are not perturbed.

5.3.7.8. Summary

The construction and operation of the VLHC present a number of ES&H challenges. Many of these have been encountered, and effectively addressed, at other accelerator facilities. Some of the problems are common to other recent projects undertaken at Fermilab and elsewhere that have resulted in the need to develop new methods to address them. Given the scale of the VLHC some of these issues may have a greater importance than found in the present experience. With adequate planning in the design stages, these problems can be adequately addressed in a manner that merits the support of the Laboratory, the Department of Energy, and the public.

References

[1] R.R. Wilson, Proceedings of Snowmass 1982.

[2] E. Malamud, ed., "The Pipetron: a Low-Field Approach to a Very Large Hadron Collider," Snowmass '96 (a.k.a. pink book).

[3] G.W. Foster, "Transmission Line Magnet Status Report," VLHC Information Packet for HEPAP Subpanel, Fermilab 1998.

[4] G.W. Foster, V.S. Kashikhin, E. Malamud, P. Mazur, H. Piekarz, J. Fuerst, R. Rabehl, P. Schlabach, J. Volk, "The 100 kA VLHC Transmission Line Magnet Superconducting Cable Test Facility," MT-16, *IEEE Trans. of Applied Superconductivity*, Vol.10, No.1, March 2000, pp.318-321.

[5] Ron Walker, 50 m Invar Thermal Cycling Report.

[6] Quench simulation final report, TD note #?

[7] J. DiMarco, G.W. Foster, V. Kashikhin, A. Makarov, P. Schlabach, "Measurements of a Crenellated Iron Pole Tip for the VLHC Transmission Line Magnet," PAC 99, pp. 3327 – 3329.

[8] G.W. Foster, V.S. Kashikhin, I. Novitski, "Design of a 2 Tesla Transmission Line Magnet for the VLHC," MT-16, *IEEE Trans. of Applied Superconductivity*, Vol.10, No.1,March 2000, pp.202-205.

[9] G.W. Foster, V.S. Kashikhin, V.V. Kashikhin, "Pole Profile Optimization of VLHC Transmission Line Magnet," EPAC 98.

[10] G.W. Foster, EPAC '98 talk and other Recycler shim talks.

[11] Kashikhin write-up on corrector wires in holes-in-the-poles.

[12] V. Tsvetkov, "Transmission Line Magnet Mechanics," TD TN *XXXX* 2001.

[13] V. Tsvetkov, "Alignment of the Transmission Line Magnet in the tunnel," TD TN XXXX 2001.

[14] V.S. Kashikhin, "Mechanical model 2 test results," TD TN XXXX. February 2001.

[15] V.S. Kashikhin, "Transmission Line Magnet for VLHC. Magnetic Forces and Magnet Deflection," TD TN XXXX. February 2001.

[16] M. McAshan, "Cryogenic System for the 3 TeV Injector Study," Fermilab TN-XXXX,1997.

[17] ULTEM 2300 is a 40% glass-filled polyetherimide marketed by GE plastics. It was developed for use in SSC quadrupole support posts at BNL. See J. Sondericker et al., *Advances in Cryogenic Engineering*, Vol. 40, pp. 1099-1105, Plenum Press, New York (1994).

[18] G.W. Foster, "Mechanical Load Cycling Tests of the Transmission Line Spiders," May 2001.

[19] I. Novitski, "Analysis of the spider support," TD TN XXXX 2001.

[20] E.C. Quimby et al., "VJR/VJRR Design, Construction, Installation, and Performance," *ACE*, vol. 43, New York, 1998.

[21] G. Grygiel et al., "Status of the TTF Cryogenic System," *ACE* vol.41, New York, 1996.

[22] K. Hosoyama et al., "Development of a High Performance Transfer Line System," *ACE* vol. 45, 2000.

[23] R. Walker et al., "Thermal Cycle Testing of Invar Pipe Welds," VLHC Note NNN.

[24] M. Chorowski, "Risk analysis of the LHC cryogenic system," ACE 2000.

[25] V. Parma et al., "The Insulation Vacuum Barrier for the Large Hadron Collider Magnet Cryostats," ICEC 18.

[26] B. Jenny et al., "A Composite Vacuum Barrier for the LHC Short Straight Section," *ACE* vol.41, New York 1996.

[27] "Technical Specification for a Compound Cryogenic Helium Distribution Line for the Large Hadron Collider (LHC)," IT-2399/lhc/lhc, Geneva, Switzerland, December 1997.

[28] R.C. Niemann, "Model SSC Dipole Magnet Cryostat Assembly at Fermilab," Supercollider 1, New York 1989.

[29] N. Andreev, TD Note.

[30] G. Ambrosio et al., "Preliminary Proposal of a Nb_3Sn Quadruple Model for the Low-Beta Insertions of the LHC," INFN Report, INFN/TC-95/25, Sept. 13, 1995.

[31] R. Scanlan, “Conductor Development Program,” Low Temperature Superconducting Workshop, Santa Rosa, CA, Nov. 8-10, 2000.

[32] M. Canali, L. Rossi, “DYNQUE: a computer code for quench simulation in adiabatic multicoil superconducting solenoids,” INFN Report, INFN/TC-93/06, 1993.

[33] L. Imbasciati, G. Ambrosio, P. Bauer, V. Kashikhin, A. Zlobin, “Quench Protection of the Common Coil Racetrack (CCRT-1): Results of Adiabatic Model Calculations,” TD-00-056, FNAL (Sept. 2000).

[34] G. Ambrosio, G. Bellomo and L. Rossi, “A 300 T/m Nb_3Sn Quadrupole for the Low-beta Insertions of the LHC,” *Proc. of EPAC96*, Sitges (Barcelona), p. 2290.

[35] Nikolai Mokhov, private communication.

[36] Bill Turner, private communication.

[37] V.V. Kashikhin, I. Terechkine, “Superconducting straight section quadrupole magnet for low-field VLHC,” FNAL, TD-01-008, Feb. 2001.

[38] Conceptual Design of the Superconducting Super Collider. SSC-SR-2020, DE93 007234.

[39] J. Volk, “Injection transfer line magnets,” TD Note TD-01-027, FNAL, 2001.

[40] J. Carson, R. Bossert, “A Proposed Production Procedure for Stage 1 Transmission Line Magnets,” TD-01-028, 2001.

[41] J. Carson, R. Bossert, “Throughput for Stage 1 Transmission Line Factory,” TD-01-029, 2001.

[42] P. Schlabach, “Magnetic Measurements During Production of VLHC Low Field Combined Function Magnets,” TD-01-007, 2001.

[43] G. Ganetis et al., “Field Measuring Probe for SSC Magnets,” Particle Accelerator Conference, 1987.

[44] L. Walkiers, “Measurements for the Acceptance Tests of the LHC Superconducting Magnets,” Eleventh International Magnet Measurement Workshop, 1999.

[45] Brown & Root, Installation & Transport Proposal for the SSC.

[46] Supply of Cryo-Magnet Transport Vehicles and Unloading Equipment for the LHC Tunnel, LHC-HMU-CI-0001 (from the CERN LHC Web site, which no longer has useful static links).

[47] An example of a commercial safety rail can be found at http://www.vahleinc.com/pdf/Catalog4C.pdf.

[48] Examples of tram systems and drive components operating in this voltage range can be found at http://w4.siemens.de/ts/products_solutions/light_rail_tram.

[49] Who?, PAC 2001 invited talk.

[50] Steve Hays, “100 kA Power Supply Options for the VLHC,” internal note (unpublished).

[51] H. Piekarz et al., “Summary of Transmission Line Magnet R&D Activities at MS-6,” VLHC Note NNNN.

[52] G.W. Foster, S. Hays, H. Pfeffer, “Design of a Compact 100 kA Switching Power Supply for Superconducting Magnet Tests,” VLHC Note NNN.

[53] J. G. Weisand (ed.), *Handbook of Cryogenic Engineering*, p. 411.

[54] K. Koepke, P. Mazur, A. Zlobin, Snowmass ’96.

[55] G.W. Foster, H. Piekarz, “Quench Protection of the Transmission Line Magnet,” VLHC note (unpublished).

[56] Switch wire is used on persistent-current MRI magnets. Commercial sources include SW-18 and SW-1 from Supercon Inc, Shrewsbury, MA, and Oxford Instruments, www.oxinst.com.

[57] See the LHC PAC ’99 papers. See also the proceeding of the workshop on powering the LHC, http://lhcp.web.cern.ch/lhcp/TCC/PLANNING/TCC/Power2000/welcome.htm.

[58] I. Terechkine, “LCW and power summary for the VLHC-1 Straight Sections,” VLHC Note NNN.

[59] Fermilab Main Injector Technical Design Report, Table 3.9.1.

[60] Typical laptop computers have heat pipes in them. See http://www.thermacore.com/papers.htm.

[61] Auto-resetting fuses are sold (for example) by: http://www.circuitprotection.com.

[62] Specifications quoted are single-quadrant DC-DC converters from Vicor, Inc. www.vicor.com.

[63] Fermilab Main Injector Note MI-75.

[64] Medvenko & Smith, Beam Instrumentation Workshop 2000, p.503.

[65] Specifications quoted are from http://products.analog.com/products/info.asp?product=AD9203.

[66] W. Turner, "Beam Tube Vacuum in Low Field and High Field Very Large Hadron Collider," LBNL-39482, UC414, presented at the Snowmass Conference, CO, October 1996.

[67] M. Pivi and W.C. Turner, "Beam Tube Vacuum in a Very Large Hadron Collider Stage 1," Version 2.1, 12 April 2001.

[68] J. Gomez-Goni, O. Gröbner and A.G. Mathewson, "Exposure of a baked Al lined stainless steel chamber to photons," CERN, Vacuum Technical Note 94-10 pg. 9, AT-VA/JGG.

[69] C. Benvenuti, "Molecular Surface pumping: the getter pumps," CAS CERN Accelerator School - Vacuum Technology, CERN Yellow Book, pg. 48.

[70] J.C. Billy, J.P. Bojon, O. Gröbner, N. Hilleret, M. Jimenez, I. Laugier, P. Strubin, "The LEP Vacuum System: a Summary of 10 Years of Successful Operation," Proc. EPAC 2000.

[71] G.P. Jackson, ed., "The Fermilab Recycler Technical Design Report", FNAL-TM-1991.

[72] I. Novitski, VLHC note on vacuum pipe stresses.

[73] A. Chao and M. Tigner, *Handbook of Accelerator Physics and Engineering*, pg.225.

[74] Oswald Gröbner pvt. comm.

[75] A. Gambitta et al., "Experience with Aluminum Vacuum Chambers at ELETTRA," EPAC 2000, Vienna, Austria; and J. Miertusova et al., "How to Save Money Designing a Vacuum System for a Third Generation Synchrotron Light Source," EPAC 1996.

[76] Bob Goodwin, Peter Lucas, Elliott McCrory and Mike Shea, "Thoughts on Controls/Instrumentation for 3 TeV booster/VLHC," http://fnalpubs.fnal.gov/archive/vlhc/VLHCPub-14.html, July 1997.

[77] V. Shiltsev, "Summary of the Working Group II: RF, Instabilities and Feedback Systems," VLHC Accelerator Technology Workshop, TJNAF, Feb.1999. http://www.vlhc.org/tjef/wg2_summary.pdf.

[78] A. Jackson, contribution to the VLHC Design Study, unpublished.

[79] The LHC Study Group, "The Large Hadron Collider – Conceptual Design Report," CERN/AC/95-05 (LHC) (1995).

[80] D. Boussard and T. Linnecar, "The LHC Superconducting RF System," *Proceedings of the 1999 Cryogenic Engineering and International Cryogenic Material Conference (CEC-ICM'99)*, 12-16 July 1999, Montreal, Canada.

[81] P. Brown et al., "Performance of the LEP200 Superconducting RF System," *Proceedings of the 9th Workshop on RF Superconductivity*, 1-5 November 1999, Santa Fe, NM, USA.

[82] P. Bosland et al., "Completion of the SOLEIL Cryomodule," *Proceedings of the 9th Workshop on RF Superconductivity*, 1-5 November 1999, Santa Fe, NM, USA.

[83] D. Boussard, "RF Power Requirements for a High Intensity Proton Collider," *Proceedings of the 1991 Particle Accelerator Conference*, pp. 2447-2449.

[84] H. Frischholz, W.R. Fowkes and C. Pearson, "Design and Construction of a 500 kW CW, 400 MHz Klystron to be Used as RF Power Source for LHC/RF Component Tests," *Proceedings of the 1997 Particle Accelerator Conference*, pp. 2911-2913.

[85] H. Padamsee, "SRF for Muon Colliders," *Proceedings of the 9th Workshop on RF Superconductivity*, 1-5 November 1999, Santa Fe, NM, USA.

[86] G. Lambertson, final report for VLHC design study (TD Note xxx).

[87] N.V. Mokhov and W. Chou, ed., "Beam Halo and Scraping," *Proc. of ICFA Workshop*, Lake Como, Wisconsin (1999).

[88] Bryant & Johnsen, *Circular Accelerators and Storage Rings*, p. 308.

[89] A.I. Drozhdin and N.V. Mokhov, "Energy Deposition Issues in the Very Large Hadron Collider," Workshop on VLHC, Fontana, Wisconsin, February 22-25, 1999.

[90] A.I. Drozhdin , N.V. Mokhov, C.T. Murphy, S. Pruss, "Beam Abort For a 50X50 TeV Hadron Collider", http://fnalpubs.fnal.gov/archive/vlhc/VLHCPub-51.ps.

[91] I.S. Baishev, A.I. Drozhdin, N.V. Mokhov, B. Parker, R.D. Richardson, J. Zhou, "Dealing with Abort Kicker Prefire in the Superconducting Super Collider," PAC 93, Washington, DC, May 1993.

[92] *The Large Hadron Collider*, Conceptual Design, CERN/AC/95-05(LHC) October 20, 1995.

[93] D.C. Wilson, C.A. Wingate, J.C. Goldstein, R.P. Godwin, N.V. Mokhov, "Hydrodynamic Calculations of 20-TeV Beam Interactions with the SSC BEAM Dump," *Proc. of IEEE Particle Accelerator Conference*, p. 3090. (1993). A legendary SSC video contains a visualization of the extracted SSC beam drilling a hole in the absorber block when the sweeping magnet system fails.

[94] N. Mokhov, pvt. comm.

[95] R. Yarema, pvt. comm.

[96] LHC Talk at Beam Instrumentation Workshop '00.

[97] S. Hunt, S. Crivello, N. Mokhov, "Radiation Effects on Optical Fiber Links at the SSC," *Nucl. Instr. Meth. in Phys. Research*, **A352** (1994) 329-243.

[98] A.I. Drozhdin and N.V. Mokhov, "The VLHC Beam Collimation System," VLHC design study note.

[99] A.I. Drozhdin, N.V. Mokhov and A.A. Sery, "The Very Large Hadron Collider Beam Collimation System," Workshop on VLHC, Fontana, Wisconsin, February 22-25, 1999.

[100] N.V. Mokhov and J.B. Strait, "Towards the Optimal LHC Interaction Region: Beam-Induced Energy Deposition," *Proc. of IEEE Particle Accelerator Conference*, p. 124 (1997).

[101] Electron Beam Tunnel Boring papers from LBL, circa 1975.

[102] "Fermilab Work Smart Standards Set," Fermi National Accelerator Laboratory, http://www-lib.fnal.gov/library/protect/worksmart.html, November 15, 1999.

[103] *United States Code of Federal Regulations, Title 10, Part 1021*, "Department of Energy National Environmental Policy Act Implementation Procedures," 1997.

[104] A. Van Ginneken, P. Yurista, and C. Yamaguchi, "Shielding calculations for multi-TeV hadron colliders," Fermilab Report FN-447 (1987).

[105] U. S. Department of Energy, "Radiation Protection of the Public and the Environment," DOE Order 5400.5, January 7, 1993.

[106] *United States Code of Federal Regulations, Title 40, Part 61, Subpart H*, "National Emissions Standard for Hazardous Air Pollutants (NESHAP) for the Emission of Radionuclides other than Radon from Department of Energy Facilities," 1989.